Carderock Division
Naval Surface Warfare Center
9500 MacArthur Blvd.
West Bethesda, MD 20817-5700

NSWCCD-70-TR--1999/163 June 1999
Signatures Directorate
Research and Development Report

CURSORY AND PRIMITIVE COMPARISON OF THE SIGNAL-TO-NOISE RATIOS OF PRESSURE AND VELOCITY PLANAR ARRAYS

by

G. Maidanik
K. J. Becker

SECURITY CLASSIFICATION OF THIS PAGE

REPORT DOCUMENTATION PAGE

Form Approved OMB No. 0704-0188

1a. REPORT SECURITY CLASSIFICATION
Unclassified

1b. RESTRICTIVE MARKINGS
None

2a. SECURITY CLASSIFICATION AUTHORITY

2b. DECLASSIFICATION/DOWNGRADING SCHEDULE

3. DISTRIBUTION / AVAILABILITY OF REPORT
Approved for public release.
Distribution is unlimited.

4. PERFORMING ORGANIZATION REPORT NUMBER(S)
NSWCCD-70-TR—1999/163

5. MONITORING ORGANIZATION REPORT NUMBER(S)

6a. NAME OF PERFORMING ORGANIZATION
Carderock Division, NSWC

6b. OFFICE SYMBOL *(if applicable)*
Code 7030

7a. NAME OF MONITORING ORGANIZATION

6c. ADDRESS *(City, State, and ZIP Code)*
9500 MacArthur Blvd.
West Bethesda, MD 20817-5700

7b. ADDRESS *(City, State, and ZIP Code)*

8a. NAME OF FUNDING/SPONSORING ORGANIZATION

8b. OFFICE SYMBOL *(if applicable)*

9. PROCUREMENT INSTRUMENT IDENTIFICATION NUMBER

8c. ADDRESS *(City, State, and ZIP Code)*

10. SOURCE OF FUNDING NUMBERS

PROGRAM ELEMENT NO.	PROJECT NO.	TASK NO.	WORK UNIT ACCESSION NO.

11. TITLE *(Include Security Classification)*
Cursory & Primitive Comparison of the Signal-to-Noise Ratios of Pressure and Velocity Planar Arrays

12. PERSONAL AUTHOR(S)
G. Maidanik, K. J. Becker

13a. TYPE OF REPORT	13b. TIME COVERED	14. DATE OF REPORT *(Year, Month, Day)*	15. PAGE COUNT
Research & Development	FROM 990501 TO 990630	1999 June 30	90

16. SUPPLEMENTARY NOTATION

17. COSATI CODES		
FIELD	GROUP	SUB-GROUP

18. SUBJECT TERMS *(Continue on reverse if necessary and identify by block number)*
Signal-to-Noise Ratio
Pressure Planar Array
Velocity Pressure Array
Turbulent Boundary Layer (TBL)

18. ABSTRACT *(Continue on reverse if necessary and identify by block number)*

A cursory and a primitive comparison between the signal-to-noise ratios of pressure and velocity arrays is conducted. The arrays of concern are planar arrays. The noise of special interest is that induced by Turbulent Boundary Layer (TBL). For a given incident pressure, as defined by its spectral density, when comparing an ideal conditioning plate (a rigid boundary) for the pressure array and an ideal conditioning compliance (a pressure release boundary) for the velocity array, the signal-to-noise ratio in the former array is by far superior to that of the latter array. A conditioning compliance that renders the boundary with an inverse fluid loading parameter that is of the order of unity may achieve for a velocity array a signal-to-noise ratio that is on par with that for the pressure array. In this comparison the two corresponding array types are subjected to the same incident spectral density.

20. DISTRIBUTION / AVAILABILITY OF ABSTRACT
☐ UNCLASSIFIED/UNLIMITED ☐ SAME AS RPT. ☐ DTIC USERS

21. ABSTRACT SECURITY CLASSIFICATION
Unclassified

22a. NAME OF RESPONSIBLE INDIVIDUAL
Maidanik, G.

22b. TELEPHONE (Including Area Code)
(301) 227-1292

22c. OFFICE SYMBOL
NSWCCD 7030

DD Form 1473, JUN 86 *Previous editions are obsolete*

SECURITY CLASSIFICATION OF THIS PAGE

Abstract

A cursory and a primitive comparison between the signal-to-noise ratios of pressure and velocity arrays is conducted. The arrays of concern are planar arrays. The noise of special interest is that induced by Turbulent Boundary Layer (TBL). For a given incident pressure, as defined by its spectral density, when comparing an ideal conditioning plate (a rigid boundary) for the pressure array and an ideal conditioning compliance (a pressure release boundary) for the velocity array, the signal-to-noise ratio in the former array is by far superior to that of the latter array. A conditioning compliance that renders the boundary with an inverse fluid loading parameter that is of the order of unity may achieve for a velocity array a signal-to-noise ratio that is on par with that for the pressure array. In this comparison the two corresponding array types are subjected to the same incident spectral density.

Introduction

Two years ago the authors issued a report entitled "Primitive comparison of the signal-to-noise ratios of pressure and velocity arrays" [1]. During this period of two years not a nibble, to use a fisherman's phrase. On the 26th of May 1999 a seminar was scheduled and delivered at NUWC, Newport, RI. In this seminar the authors had the opportunity to introduce, directly to a scientific community at large, the material contained in the referenced report. Of course, inspite of the time constraint, modifications to the referenced report and some new material were introduced to fit the specific purpose of the seminar. The purpose included reaching an audience that is more directly concerned with the possible application of the subject matter. After the seminar was presented, it was decided to issue at this juncture a companion report to the referenced report. This companion report is to be based on the format in which the material was presented at the seminar. In this vein the viewgraphs are placed on the right of a two-sided report. When called for, on the left-side a few comments regarding the viewgraph on the right are to be presented. In this way the report has a seminar-like flavor. It is hoped that the flavor may be palatable to most readers. Above all, this companion report may remove a great number of infuriating typos that inadvertently permeate any report and any viewgraph; this removal may in itself justify the publication of this companion report.

For a given incident pressure, as defined by its spectral density, when comparing an ideal conditioning plate (a rigid boundary) for the pressure array and an ideal conditioning compliance (a pressure release boundary) for the velocity array, the signal-to-noise ratio in the former array is by far superior to that in the latter array. It transpires that a conditioning compliance that renders the boundary with an inverse fluid loading parameter (ε_o) that is of the order of unity may achieve for a velocity array a signal-to-noise ratio that is on par with a pressure array. The parameter (ε_o) $[= K_o/(\omega_o \rho c)]$ relates the surface stiffness (K_o) of the conditioning compliance to the characteristic impedance (ρc) of the fluid. This relationship defines the resonance frequency (ω_o) of the surface stiffness of the compliant layer with the surface mass of the fluid. In this *on par* equality the two arrays are subjected to the same incident spectral density. This achievement for the velocity array is predicated on a resonance condition as just stated. Therefore, the equality appears destined to be confined to a narrow frequency band. In this report, however, the conditioning compliance is implemented by merely placing a simple

compliant layer on a well nigh rigid backing plate. Of course, the conditioning compliance describes, in a general context, a boundary on which the mechanical surface impedance is suitably designed. A suitable boundary of relevance in this report is a boundary that resonates with the surface mass of the fluid atop. If this resonance condition can be sustained over a wider frequency band, the conditioning compliance is correspondingly of a wider frequency band. Such boundaries may be designed by a more elaborate compliant layer and/or by a more compounded combination of surface stiffnesses and surface masses and/or by even some non-mechanical elements thrown in. In a recent report describing another device that is based upon a resonance, the conditions that are necessary to maintain and sustain the resonance over a wider frequency band were introduced [2]. Whether an analogous widening of the frequency band may be achieved for the device of focus here is yet to be ascertained.

Viewgraph 2

Since the surface impedance of the boundary, with the array in place, is idealized to be spatially and temporally uniform, only specular reflections exist; the boundary does not cause any wavevector (and frequency) conversions [3]. Then, if the incident pressure is uniform, both in the spatial vector domain and in the temporal domain, the pressure on the boundary retains this characterization.

The equation of the conservation of momentum at the fluid-boundary interface is differential in the spatial-temporal domain. This equation is algebraic in the corresponding spectral domain. Then, a fluid-surface impedance; the quantity $Z_w(k,\omega)$, may be algebraically defined in terms of the pressure and the velocity on the boundary.

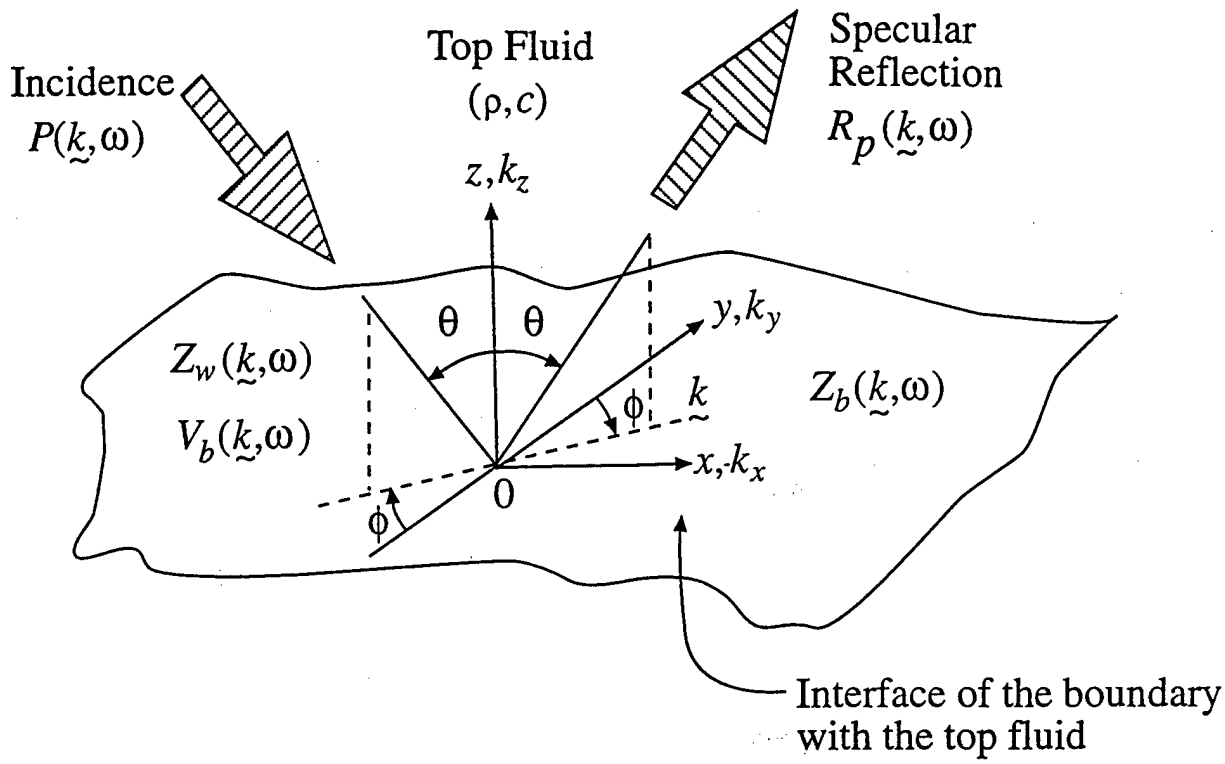

The pressure p_b and the velocity v_b on the boundary are related, in terms of the conservation of momentum at the fluid-boundary interface, in the form

$$\rho(\partial v_b / \partial t) = -(\partial p_b / \partial z) ,$$

where (ρ) is the fluid density, (t) is the temporal variable and (z) is the spatial variable normal to the boundary. In spectral space

$$[P_b(\underset{\sim}{k},\omega) / V_b(\underset{\sim}{k},\omega)] = Z_w(\underset{\sim}{k},\omega) = (\rho c / \bar{k}_z) ;$$

$k_z = (\omega / c)\bar{k}_z$, (c) = speed of sound in the fluid.

Viewgraph 3

The wave equation renders the normalized wavenumber $(\bar{k}_z)$ positive and real in the supersonic range and negative and imaginary in the subsonic range, where (U) is the usual unit step function; namely

$$U(a) = \begin{cases} 1 \ , & a>0 \\ 0 \ , & a<0 \end{cases} \quad .$$

$P_b(\underset{\sim}{k},\omega)$ and $V_b(\underset{\sim}{k},\omega)$ now obey the wave equation and $Z_w(\underset{\sim}{k},\omega)$ is the fluid-surface impedance in the plane of the boundary. Since the boundary is uniform, the relationship between $P_b(\underset{\sim}{k},\omega)$ and $V_b(\underset{\sim}{k},\omega)$ is the same as between the incident pressure $P(\underset{\sim}{k},\omega)$ and the incident velocity $V(\underset{\sim}{k},\omega)$. Thus

$$\Phi_v(\underset{\sim}{k},\omega) = E_p^v(\underset{\sim}{k},\omega)\,[\Phi_p(\underset{\sim}{k},\omega)/(\rho c)^2]$$

$$\Phi_p(\underset{\sim}{k},\omega) = |P(\underset{\sim}{k},\omega)|^2 \quad ; \quad \Phi_v(\underset{\sim}{k},\omega) = |V(\underset{\sim}{k},\omega)|^2$$

are just as valid as the relationships on the viewgraph.

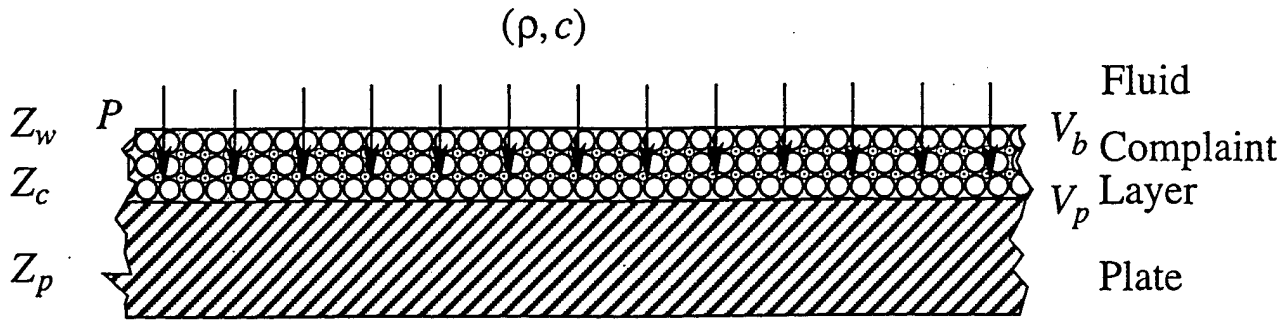

The wave equation in the fluid demands

$$\bar{k}_z \Rightarrow \bar{k}_3 = [1-(kc/\omega)^2]^{1/2} U\ [1-(kc/\omega)]$$

$$-i[(kc/\omega)^2 - 1]^{1/2}\ \ U[(kc/\omega)-1]\ ; \quad |\underset{\sim}{k}| = k \quad ,$$

$$[P_b(\underset{\sim}{k},\omega)/V_b(\underset{\sim}{k},\omega)] \Rightarrow Z_w(k,\omega)\ ;\ \ Z_w(\underset{\sim}{k},\omega) = (\rho c/\bar{k}_3)$$

Spectral density

$$\Phi_{bv}(\underset{\sim}{k},\omega) = E_p^v(\underset{\sim}{k},\omega)[\Phi_{bp}(\underset{\sim}{k},\omega)/(\rho c)^2]\ ;$$

$$E_p^v(\underset{\sim}{k},\omega)\ =\ |1-kc/\omega)^2|\ ,$$

where

$$\Phi_{bp}(\underset{\sim}{k},\omega) = |P_b(\underset{\sim}{k},\omega)|^2\ ;\ \Phi_{bv}(\underset{\sim}{k},\omega) = |V_b(\underset{\sim}{k},\omega)|^2\ .$$

Viewgraph 4

The validity of the equivalent circuit diagram again is predicated on the uniformity of the surface impedances involved, so that they can be represented by lump parameters and the relationships among them are algebraic. Of course one may readily introduce compliant layers that are wavevector dependent; i.e., $K = K(\underset{\sim}{k}, \omega)$, and orthotropy in both, in the plates and in the compliant layers, may also be readily introduced. However, in this report, for the sake of simplicity, such introductions are not explicitly considered. Moreover, in subsequent computations only the two approximations to the surface impedance of the boundary $Z_b(\underset{\sim}{k}, \omega)$; namely $Z_p(\underset{\sim}{k}, \omega)$ or $Z_c(\underset{\sim}{k}, \omega)$, are imposed. The generalization to the more elaborate form of the surface impedance is readily implemented and computed. Again, for the sake of simplicity computations including these generalizations are not implemented in the material to be presented herein.

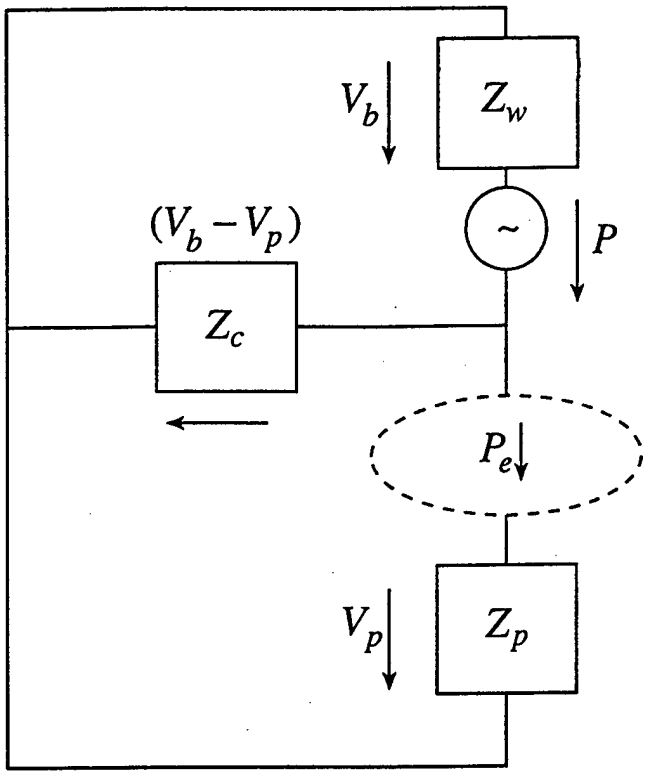

$$Z_b = (Z_c Z_p)(Z_c + Z_p)^{-1} \simeq \begin{cases} Z_p \; ; & |Z_c| >> |Z_p| \\ Z_c \; ; & |Z_c| << |Z_p| \end{cases} .$$

$$Z_p(\underset{\sim}{k},\omega) = i\omega m[1-(|\underset{\sim}{k}|/k_p)^4(1+(\eta_p)] \; ; \; k_p^2 = (\omega\omega_c/c^2) ,$$

$$Z_c(\underset{\sim}{k},\omega) = (K/i\omega) \; ; \; K = K_o(1+i\eta_o) ,$$

$$[P_b(\underset{\sim}{k},\omega)/V_b(\underset{\sim}{k},\omega)] = Z_w(\underset{\sim}{k},\omega) = (\rho c/\bar{k}_3) \; ;$$

$$\bar{k}_3 = \bar{k}_3(\underset{\sim}{k},\omega) = [1-(kc/\omega)^2]^{1/2} U[1-(kc/\omega)]$$

$$-i[(kc/\omega)^2 - 1]^{1/2} U[(kc/\omega)-1] .$$

The incident pressure on a boundary is spatially and temporally stationary so that the pressure can be defined in terms of its spectral density $\Phi(\underset{\sim}{k},\omega)$, where $(\underset{\sim}{k})$ is the wave vector variable in the plane of the boundary and (ω) is the frequency variable. It is also assumed that the spectral components in the signal are uncorrelated with the spectral components of the (unwanted) noise so that

$$\Phi(\underset{\sim}{k},\omega)=\Phi_S(\underset{\sim}{k},\omega) + \Phi_N(\underset{\sim}{k},\omega) \; ; \quad \underset{\sim}{k} = \{k_x, k_y\} \; ,$$

where $\Phi_S(\underset{\sim}{k},\omega)$ and $\Phi_N(\underset{\sim}{k},\omega)$ are the spectral densities of the signal and the noise, respectively.

Viewgraph 6

The steered filtering efficiency $A(\underset{\sim}{k}_s|\underset{\sim}{k},\omega)$ implicitly accounts for a frequency efficiency filtering. In certain situations the frequency filtering efficiency plays a major role in the filtering efficiency of the array. In this report the frequency filtering efficiency of the array is idealized in the form

$$A(\underset{\sim}{k}_s|\underset{\sim}{k},\omega)\Phi(\underset{\sim}{k},\omega) \equiv \int d\omega' A'(\underset{\sim}{k}_s|\underset{\sim}{k},\omega\,|\,\omega')\ \Phi(\underset{\sim}{k},\omega') \quad ,$$

where in particular and as an example

$$A'(\underset{\sim}{k}_s|\underset{\sim}{k},\omega\,|\,\omega') \ \equiv \ A(\underset{\sim}{k}_s|\underset{\sim}{k},\omega)\ \delta(\omega-\omega') \quad .$$

In this format (ω) designates a specific frequency. In that context the variation in that specific frequency defines a frequency variable in the spectral density $\Phi(\underset{\sim}{k},\omega)$.

The output $O(\underset{\sim}{k}_s,\omega)$ of the boundary array to the incident spectral density $\Phi(\underset{\sim}{k},\omega)$ may be formally expressed in the form

$$O(\underset{\sim}{k}_s,\omega)=\int d\underset{\sim}{k}\;\; J(\underset{\sim}{k}_s|\underset{\sim}{k},\omega)\Phi(\underset{\sim}{k},\omega)\;;\quad d\underset{\sim}{k}=dk_x dk_y\;;$$

$$J(\underset{\sim}{k}_S|\underset{\sim}{k}\,\omega)\;=\;A(\underset{\sim}{k}_S|\underset{\sim}{k},\omega)D(\underset{\sim}{k},\omega)\;;\qquad \underset{\sim}{k}_S=\{k_{sx},k_{sy}\}\;,$$

where $D(\underset{\sim}{k},\omega)$ is the filtering efficiency of the boundary -- the passive filtering efficiency—and $A(\underset{\sim}{k}_s|\underset{\sim}{k},\omega)$, is the filtering efficiency of the array -- the steered filtering efficiency--steered to the specific wave vector ($\underset{\sim}{k}_s$). The quantity $J(\underset{\sim}{k}_s|\underset{\sim}{k},\omega)$ is the combined filtering efficiency of the flush mounted array.

Viewgraph 7

Again, the frequency variable (ω) and the frequency filtering efficiency is as defined in the previous viewgraph; i.e., Viewgraph 6.

Both the passive and the steered filtering efficiencies are designed into the array in order to maximize the signal-to-noise ratio R_N^S, which is given by

$$R_N^S(\underset{\sim}{k}_S,\omega) = [O_S(k_S,\omega) \,/\, O_N(\underset{\sim}{k}_S,\omega)] \,,$$

$$O_S(\underset{\sim}{k}_S,\omega) = \int d\,\underset{\sim}{k}\; A(\underset{\sim}{k}_S \mid \underset{\sim}{k},\omega)\; D(\underset{\sim}{k},\omega)\; \Phi_S(\underset{\sim}{k},\omega) \,,$$

$$O_N(\underset{\sim}{k}_S,\omega) = \int d\,\underset{\sim}{k}\; A(\underset{\sim}{k}_S \mid \underset{\sim}{k},\omega)\; D(\underset{\sim}{k},\omega)\; \Phi_N(\underset{\sim}{k},\omega) \,.$$

The maximization of R_N^S requires the combined filtering efficiency $J(\underset{\sim}{k}_S \mid \underset{\sim}{k},\omega)$ $\{=[A(\underset{\sim}{k}_S \mid \underset{\sim}{k},\omega)\; D(\underset{\sim}{k},\omega\,]\}$ to favorably accept the signal components $\Phi_S(\underset{\sim}{k},\omega)$ and to simultaneously reject the noise components $\Phi_N(\underset{\sim}{k},\omega)$.

Viewgraph 8

$$U(a) = \begin{cases} 1 \ , & a > 0 \\ 0 \ , & a < 0 \end{cases} .$$

For example, it is a fact that the signal $\Phi_S(\underset{\sim}{k},\omega)$ is supersonic; i.e.,

$$\Phi_S(\underset{\sim}{k},\omega) \;=\; \Phi_{0S}(\underset{\sim}{k},\omega)\;\; U\;\; [1-(kc/\omega)]\;,$$

where U is the unit step function and $k \;=\; |\underset{\sim}{k}|$. It becomes necessary, therefore, to ensure that the combined filtering efficiency $J(\underset{\sim}{k}_S \,|\, \underset{\sim}{k},\omega)$ is supersonically viable.

On the other hand, the noise $\Phi_N(\underset{\sim}{k},\omega)$ possesses, by definition, subsonic components in the incident spectral density on the boundary as well as supersonic components:

$$\Phi_N(\underset{\sim}{k},\omega) = \Phi_{0N}(\underset{\sim}{k},\omega)\ U[1-(kc/\omega)] + \Phi_{1N}(\underset{\sim}{k},\omega)U[(kc/\omega)-1]\ .$$

The combined filtering efficiency $J(\underset{\sim}{k}_s \mid \underset{\sim}{k},\omega)$ is the better the more it rejects subsonic components. That betterment, however, should not be derived at the expense of the acceptance in the supersonic range. The supersonic components in the noise; namely, $\Phi_{0N}(\underset{\sim}{k},\omega)\ U[1-(kc/\omega)]$, are not readily distinguishable from those of the signal.

Viewgraph 10

A sophistication may, for example, involve adaptive steering.

To selectively make this distinction between these two types of supersonic components; the supersonic signal components and the supersonic noise components, the steered filtering efficiency $A(\underset{\sim}{k}_s \mid \underset{\sim}{k}, \omega)$ must attain a degree of sophistication, notwithstanding that this filtering efficiency may be called upon to further enhance the rejection of the subsonic components above and beyond that provided by the passive filtering efficiency $D(\underset{\sim}{k}\,\omega)$.

The foregoing is intended to serve merely as a review of material assumed familiar to the reader. The present seminar attempts to contrast the performance of two array types. One is composed of embedded "pressure transducers" that are flush mounted in the boundary and the second of "velocity transducers." Both arrays are assumed to be subjected to the same incident pressure spectral density $\Phi_p(\underset{\sim}{k},\omega)$. However, each array is designed to maximize the signal-to-noise ratio $R_N^S(\omega)$; $R_{pN}^S(\omega)$ for the pressure array and $R_{vN}^S(\omega)$ for the velocity array.

The dependence of the spectral densities on $\underset{\sim}{k}_s$ and $\underset{\sim}{k}$ are depicted in terms of the wavenumbers $k_s(=|\underset{\sim}{k}_s|)$ and $k(=|\underset{\sim}{k}|)$. The two dimensional character of the spectral densities of the signal and the noise are more closely sketched in the figure below. This figure shows a possible realization of these spectral densities.

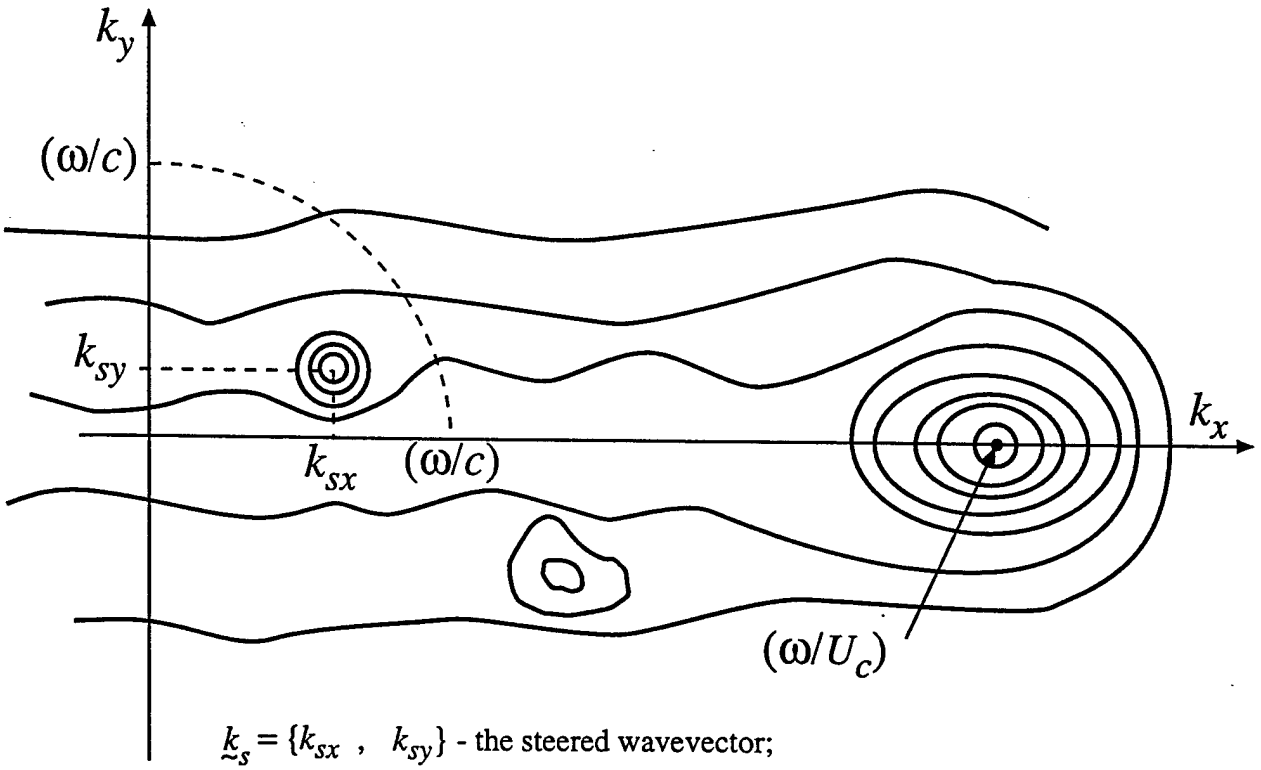

$\underset{\sim}{k}_s = \{k_{sx}\ ,\ k_{sy}\}$ - the steered wavevector;

c - the sound speed in the fluid;

U_c - the convective speed of a TBL.

The reader is asked to conjure the difference and accept the limitation in the presentation on the viewgraph; a two-dimensional representation is projected on a one-dimensional counterpart. The sketch may help some readers to better visualize the intended meaning of the less detailed presentation used in this and the two following viewgraphs; Viewgraphs 13 and 14.

Hypothetical but instructive illustrations of

a. The spectral densities of the signal and the noise.

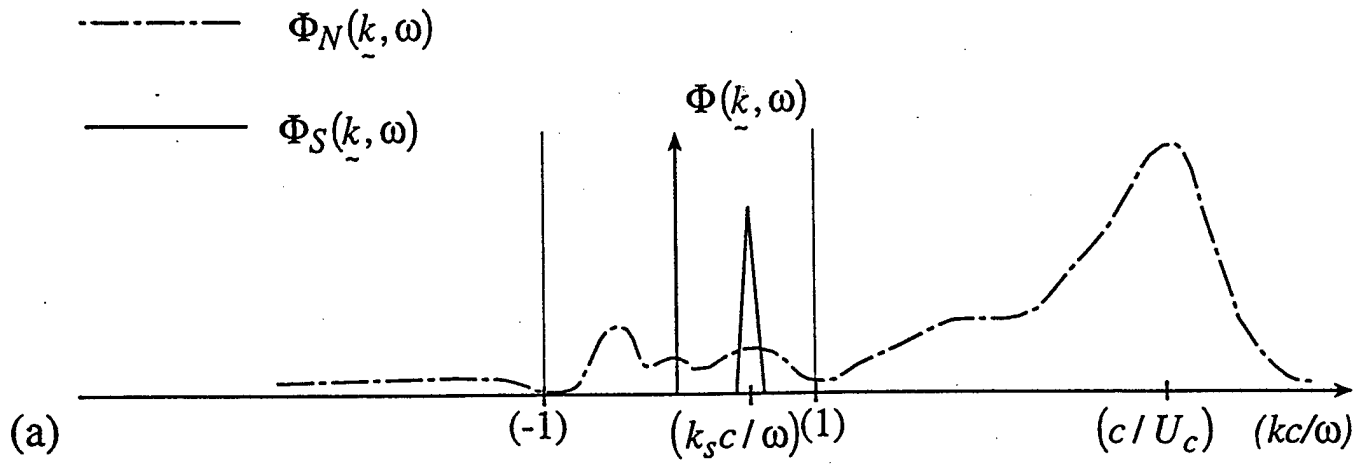

Viewgraph 13

The comments made with respect to the preceding viewgraph (Viewgraph 12) are relevant to this viewgraph.

Hypothetical but instructive illustrations of the filtering efficiencies $A(\underset{\sim}{k}_s|\underset{\sim}{k},\omega)$ and $D(\underset{\sim}{k},\omega)$ and their utility are sketched on this viewgraph.

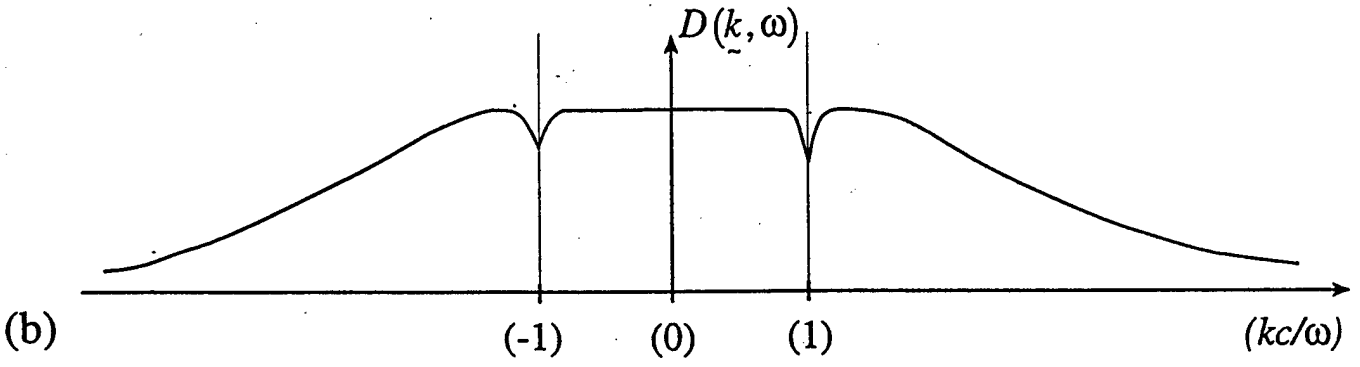

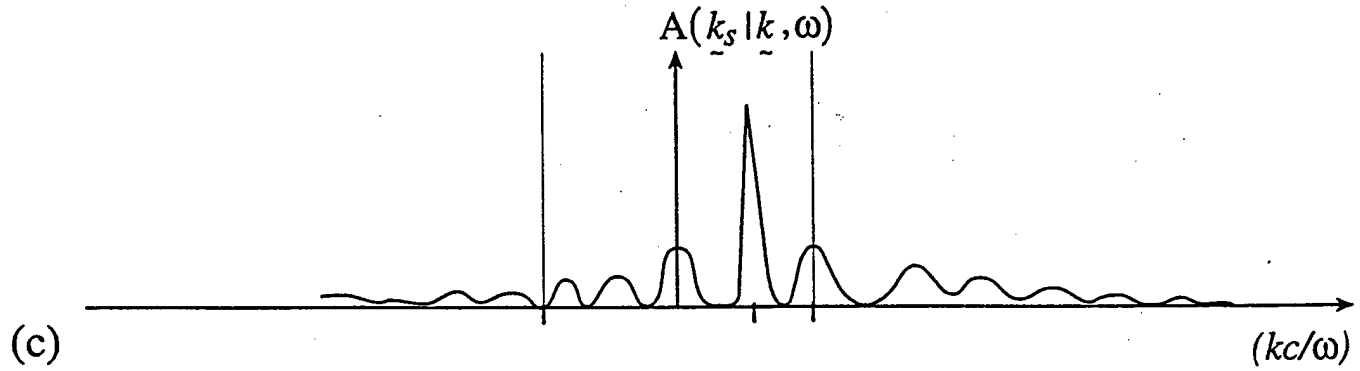

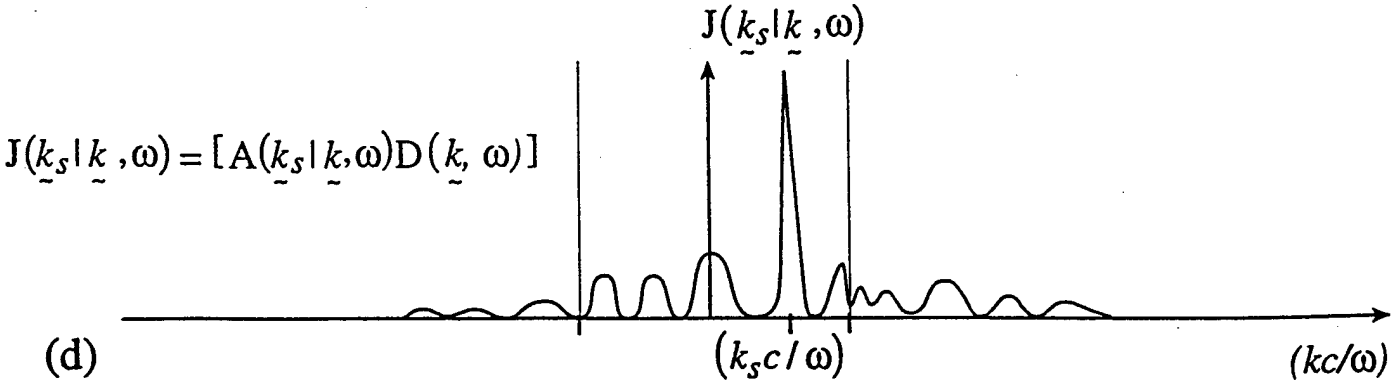

a. The spectral densities of the signal and the noise.

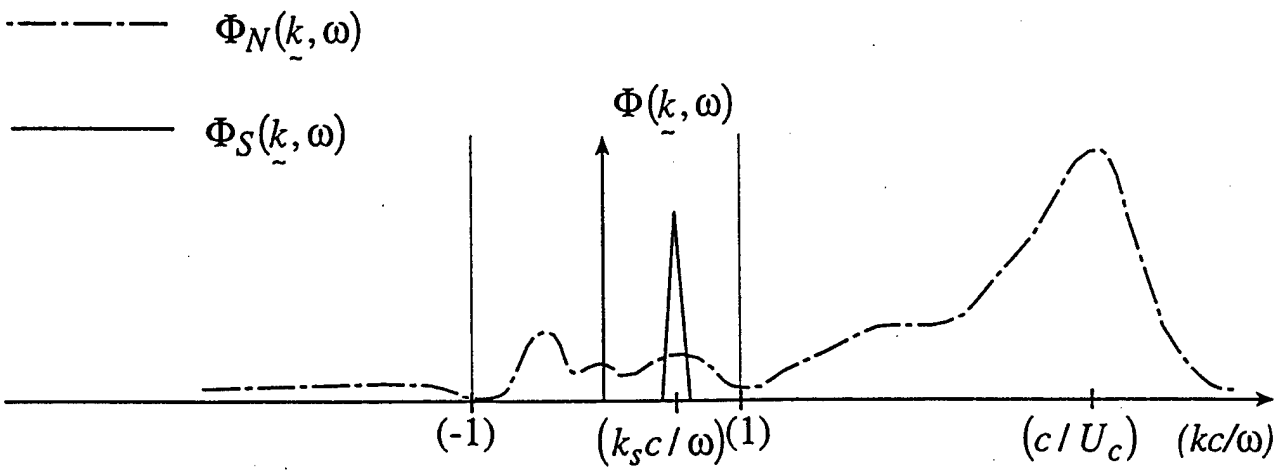

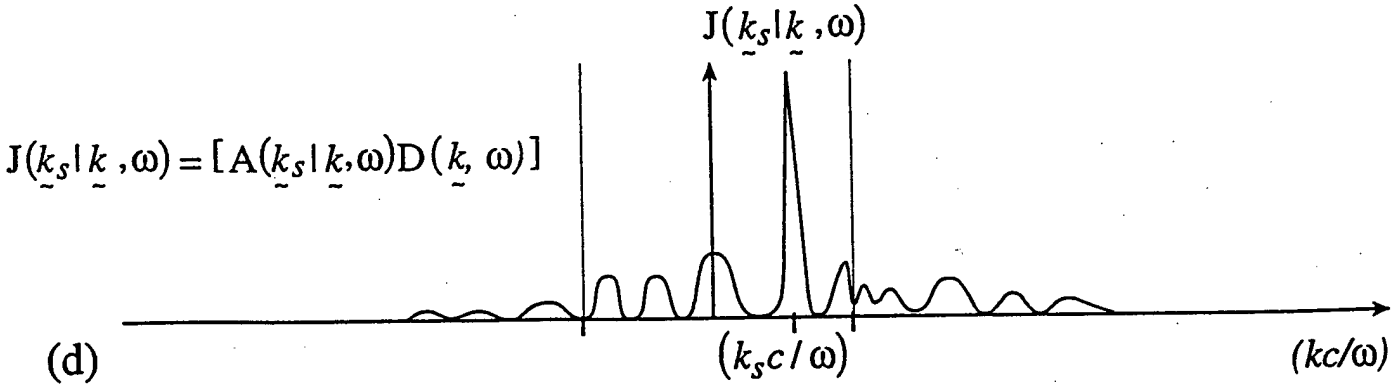

d. The combined filtering efficiency of the array.

Viewgraph 15

In this report the surface impedances that are involved at the boundary are assumed to be isotropic and, hence, the passive filtering efficiencies are, in fact, dependent on the wavenumber (k) and not on the wavevector $(\underset{\sim}{k})$. In this sense, the factors in the passive filtering efficiencies may be naturally depicted in terms of the normalized wavenumber (kc/ω); the values of these factors are assumed to be independent of the angular variables.

Passive Filtering Efficiency for a Pressure Array

The incident pressure $P(\underset{\sim}{k},\omega)$ on the boundary is presented to the boundary as

$$P_b(\underset{\sim}{k},\omega) \;=\; P(\underset{\sim}{k},\omega)[1+R_p(\underset{\sim}{k},\omega)]\ ,$$

where $R_p(\underset{\sim}{k},\omega)$ is the boundary reflection coefficient

$$R_p(\underset{\sim}{k},\omega)=[Z_b(\underset{\sim}{k},\omega)-Z_w(\underset{\sim}{k},\omega)]\ [Z_b(\underset{\sim}{k},\omega)+Z_w(\underset{\sim}{k},\omega)]^{-1}$$

and $Z_b(\underset{\sim}{k},\omega)$ is the mechanical surface impedance of the boundary; e.g., for a boundary that is equivalently a thin isotropic plate responding in flexure

$$Z_b(\underset{\sim}{k},\omega)\Rightarrow Z_p(\underset{\sim}{k},\omega)=i\omega m[1-(k/k_p)^4(1+i\eta_p)],$$

with $k_p^2=[\omega\omega_c/c^2]$ and $Z_w(\underset{\sim}{k},\omega)=[(\rho c)/\bar{k}_3]$.

The factor $[1+R_p(\underset{\sim}{k}\,\omega)]$ is the "conditioning plate" filtering function; the filtering efficiency $C_p(\underset{\sim}{k},\omega)$ of the conditioning plate is then given by

$$C_p(\underset{\sim}{k},\omega) \;=\; |1+R_p(\underset{\sim}{k},\omega)|^2$$

$$\;=\; 4\,|Z_p(\underset{\sim}{k},\omega)|^2\,|Z_p(\underset{\sim}{k},\omega)+Z_w(\underset{\sim}{k},\omega)|^{-2}\ .$$

Viewgraph 16a

An ideal conditioning plate is one for which $|Z_p(\underset{\sim}{k},\omega)| >> |Z_w(\underset{\sim}{k},\omega)|$ throughout the relevant spectral space of concern. The inequality can hardly be maintained at and in the vicinity of the sonic region where $(kc/\omega)=1$. In this sonic region the fluid-surface impedance $Z_w(\underset{\sim}{k},\omega)$ assume absolute values that are far in excess of the characteristic fluid impedance (ρc). Then no reasonable plate-surface impedance can compete with such values. Nonetheless, the ideal conditioning plate, except for that sonic region, induces passive filtering efficiency $C_p(\underset{\sim}{k},\omega)$ that is maintained at the value of (4), as depicted in the viewgraph. In the viewgraph

$$[(\rho c)/(\omega m)] = [\varepsilon_c(\omega_c/\omega)] << 1 \;\; ; \;\; \varepsilon_c << 1 << (\omega_c/\omega) \;\; ,$$

where (m) is the surface mass associated with the plate and (ω_c) is the critical frequency of the plate with respect to the speed of sound in the fluid. This inequality ensures that the plate surface impedance $Z_p(\underset{\sim}{k},\omega)$ on the dominating surface impedance on the boundary in the spectral region of concern. This dominance is even with respect to the fluid-surface impedance. To validate the above inequality in the viewgraph one requires (ω_c/ω) to be at least (10^6) and the fluid loading parameter (ε_c) to be less than (10^{-6}). Only an ideal conditioning plate (an essentially rigid plate) may sustain such extreme values.

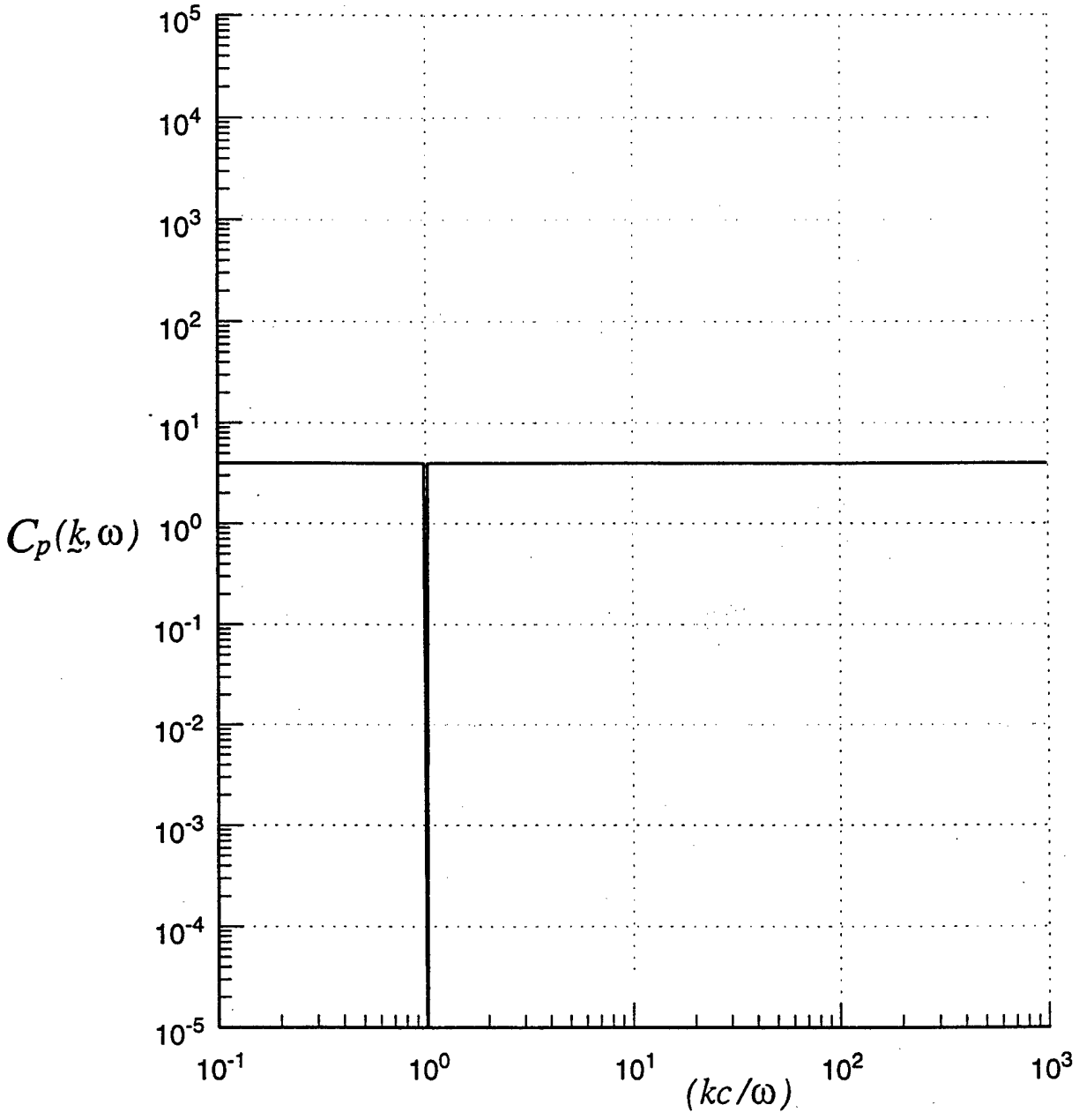
$C_p(\underline{k},\omega)$
10^5
10^4
10^3
10^2
10^1
10^0
10^{-1}
10^{-2}
10^{-3}
10^{-4}
10^{-5}
10^{-1}
10^0
10^1
10^2
10^3
(kc/ω)

Viewgraph 16b

In this viewgraph the passive filtering efficiency $C_p(\underset{\sim}{k},\omega)$ is compared with the ideal when the inequality

$$[(\rho c)/(\omega m)] \;=\; \varepsilon_c(\omega_c/\omega) \;<<\; 1$$

stands in violation. Two cases that stand in violation are depicted on this viewgraph. Although the violation in both cases is to the same extent, the results are different; i.e., the product $[\varepsilon_c(\omega_c/\omega)]$ is the same in the two cases, the difference lies in that (ε_c) and (ω_c/ω) are not equal in the two cases. Since the "anti-resonance" and the "resonance" that follows are due to the small value of $|Z_p(\underset{\sim}{k},\omega)|$ and due to the surface stiffness of the plate resonating with the surface mass of the fluid, respectively, the positioning of the anti-resonance and resonance are readily ascertained; e.g., the anti-resonance occurs at $(kc/\omega) \simeq (\omega_c/\omega)^{1/2}$. There is a loss in the pressure doubling that the ideal conditioning plate sustains. This is manifest by a departure of $C_p(\underset{\sim}{k},\omega)$ below the resonance from the value of (4). The decrease in the passive filtering efficiency is rendered by the higher ratio of the fluid-surface impedance to the surface impedance of the conditioning plate. This higher ratio is reflected by a higher $[(\rho c)/(\omega m)]$ in the spectral range preceding the resonance. Indeed, since the ratio $[(\rho c)/(\omega m)]$ is the same in the two cases, $C_p(\underset{\sim}{k},\omega)$ is diminished equally in the two cases in the relevant range of (kc/ω). Above the resonance condition, where $(kc/\omega) > (\omega_c/\omega)^{1/2}$, the surface impedance of the conditioning plate in the two cases becomes totally dominant on the boundary and $C_p(\underset{\sim}{k},\omega)$ assumes the value of (4). [cf. Viewgraph 16a.]

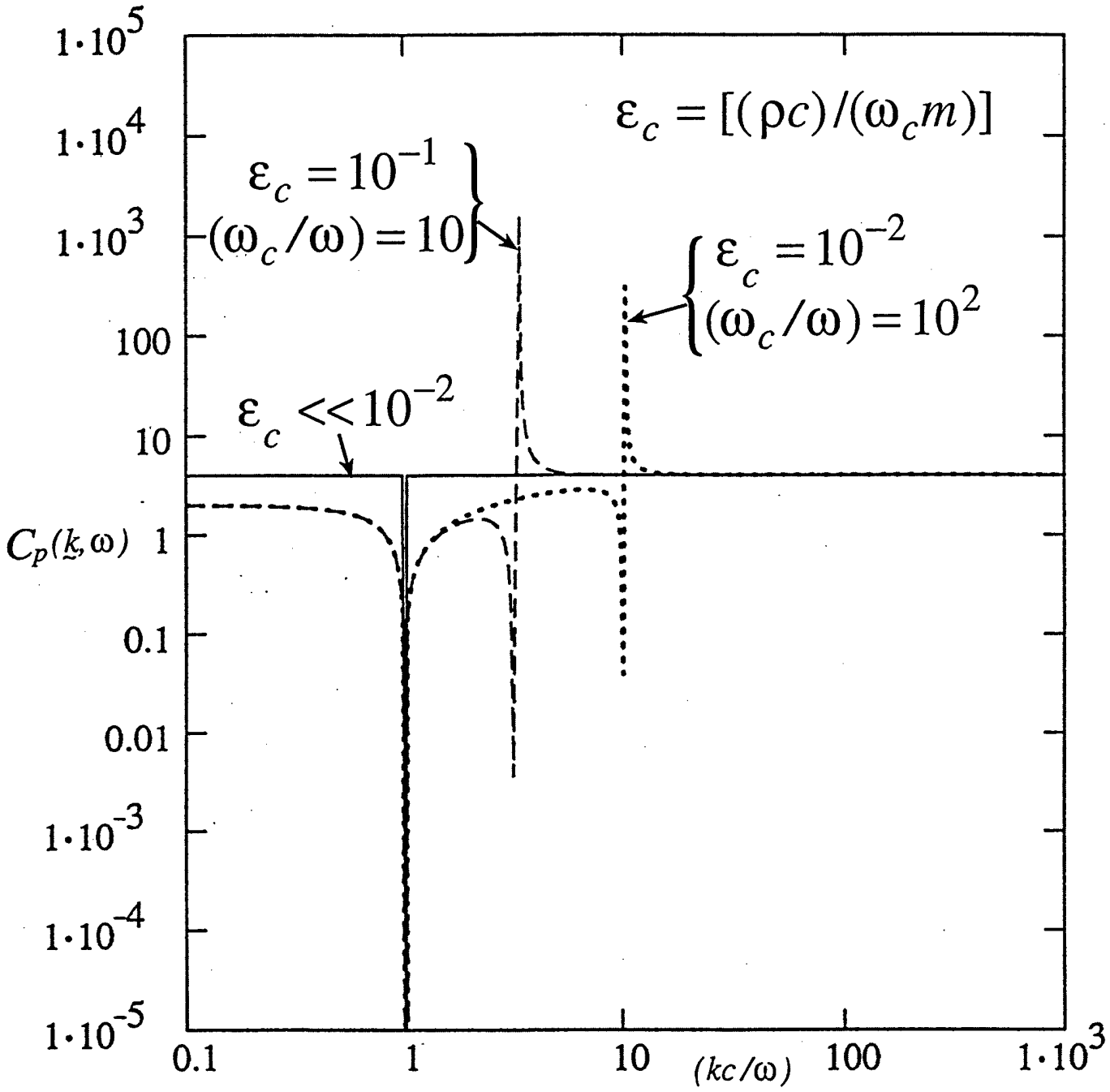

Resonance of surface stiffness of plate and surface mass of fluid

Viewgraph 17

A device that assists the passive filtering efficiency of a boundary is to place a blanket over the array; the blanket removes the interface with the fluid to the surface atop the blanket. The blanket is assumed to be endowed with a fluid-like properties in that it transmits intact the supersonic components and it decays exponentially the subsonic components on their way from the top surface onto the array boundary at the bottom surface of the blanket. The exponential decay is governed by the thickness of the blanket in the manner stated in the equation in the viewgraph. Unlike the fluid, however, the blanket retains its shape in lieu of its shear modulus that is ignored in the ideal blanket here considered. The filtering efficiency $B(\underset{\sim}{k},\omega)$ of an ideal blanket constitutes a factor in the passive filtering efficiency $D(\underset{\sim}{k},\omega)$ of the array. The nature of the factor $B(\underset{\sim}{k},\omega)$ of an ideal blanket is depicted in the viewgraph. Since only the subsonic components are decayed by a blanket, it assists the passive filtering efficiency to cope with noise components in that spectral range. The blanket is neutral in the supersonic range; it does not assist the passive filtering efficiency of the array to distinguish between supersonic components that belong to the signal and to the noise.

The filtering efficiency $B(\underset{\sim}{k},\omega)$ of a blanket

$$B(\underset{\sim}{k},\omega) = U[1-(kc/\omega)]$$

$$+\exp[-2(b\omega/c)\{(kc/\omega)^2-1\}^{1/2}]\ U[(kc/\omega)-1]$$

where (b) is the thickness of the blanket.

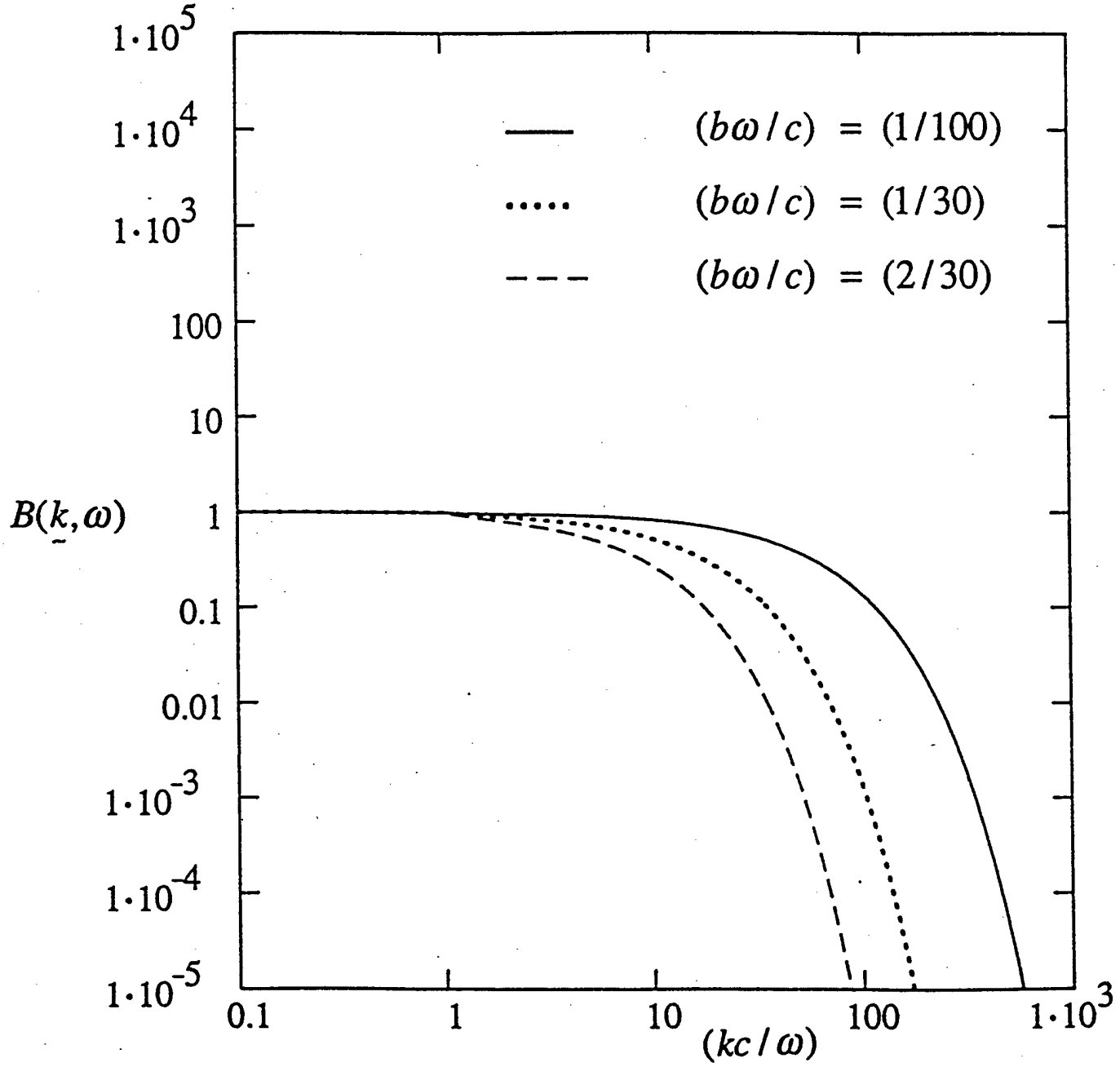

Viewgraph 18a

This viewgraph depicts the passive filtering efficiency $D_p(\underset{\sim}{k},\omega)$ of a pressure array incorporating an ideal conditioning plate and a standard blanket. The passive filtering efficiency $C_p(\underset{\sim}{k},\omega)$ for the ideal conditioning plate is depicted in viewgraph 16a and the passive filtering efficiency $B(\underset{\sim}{k},\omega)$ for the standard blanket is depicted in Viewgraph 17. (The standard blanket is characterized by a thickness $(b\omega/c) = (1/30)$.)

$$D_p(\underset{\sim}{k},\omega) = C_p(\underset{\sim}{k},\omega)B(\underset{\sim}{k},\omega) \ .$$

Comparing Viewgraph 18a with Viewgraph 16a reveals the effectiveness of the blanket with respect to the noise. One is merely reminded that spectral density components that reside in the subsonic range are noise components. The higher the subsonic range the more effective is the blanket. The spectral density components that reside in the supersonic range are unaffected by the presence of the blanket, whether the components are signal or noise.

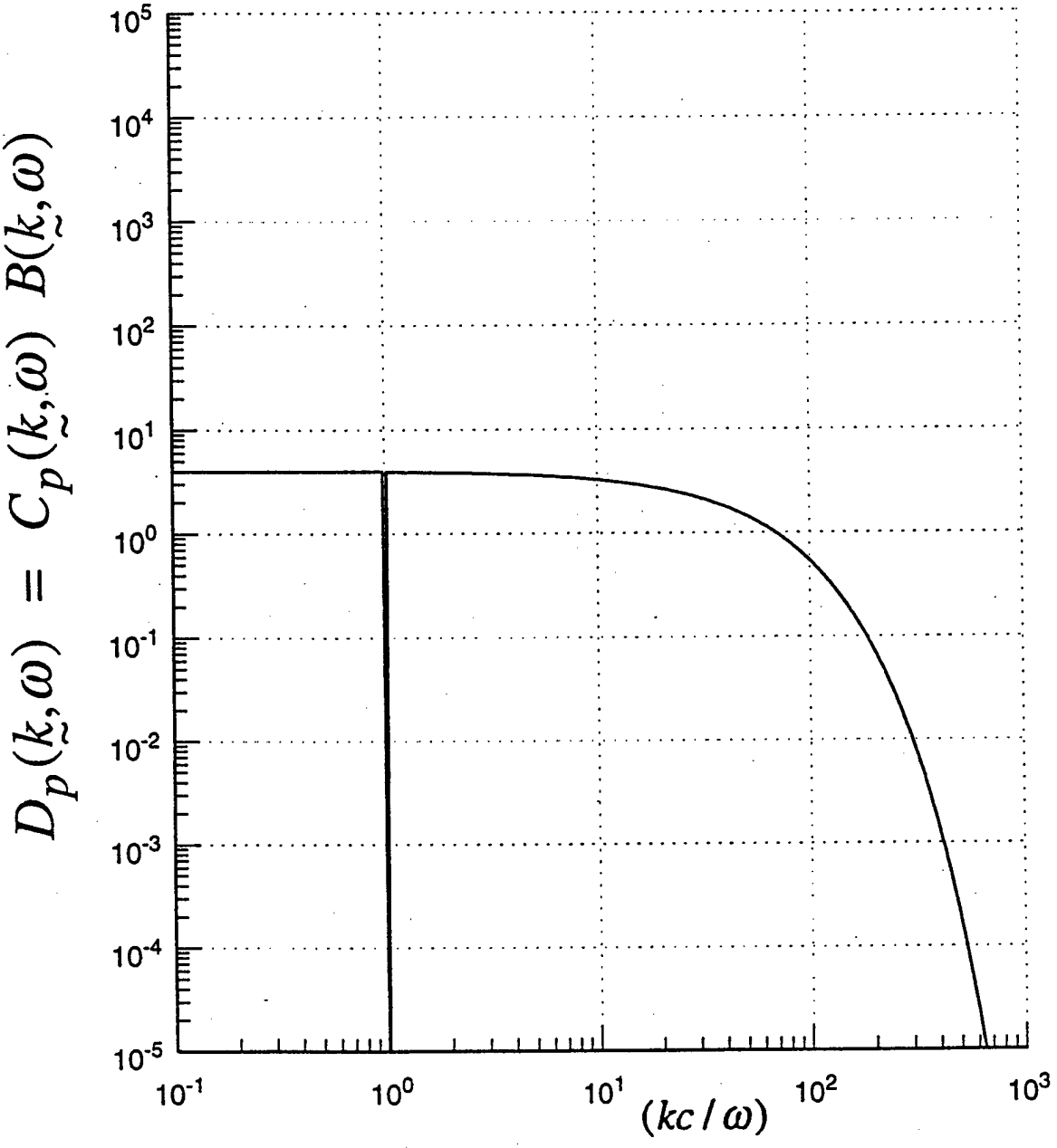
$D_p(\underset{\sim}{k},\omega) \equiv C_p(\underset{\sim}{k},\omega)\ B(\underset{\sim}{k},\omega)$
10^5
10^4
10^3
10^2
10^1
10^0
10^{-1}
10^{-2}
10^{-3}
10^{-4}
10^{-5}
10^{-1}
10^0
10^1
10^2
10^3
(kc/ω)

Viewgraph 18b

Again, in this viewgraph the passive filtering efficiency $B(\underset{\sim}{k},\omega)$ is that of the standard blanket. This viewgraph is composed of data presented in Viewgraphs 16 and 17.

The passive filtering efficiency $D_p(\underset{\sim}{k},\omega)$ for the pressure array is the combined passive filtering efficiency $C_p(\underset{\sim}{k},\omega)$ of the conditioning plate and the passive filtering efficiency $B(\underset{\sim}{k},\omega)$ of the blanket; namely $D_p(\underset{\sim}{k},\omega) = C_p(\underset{\sim}{k},\omega)\ B(\underset{\sim}{k},\omega)$.

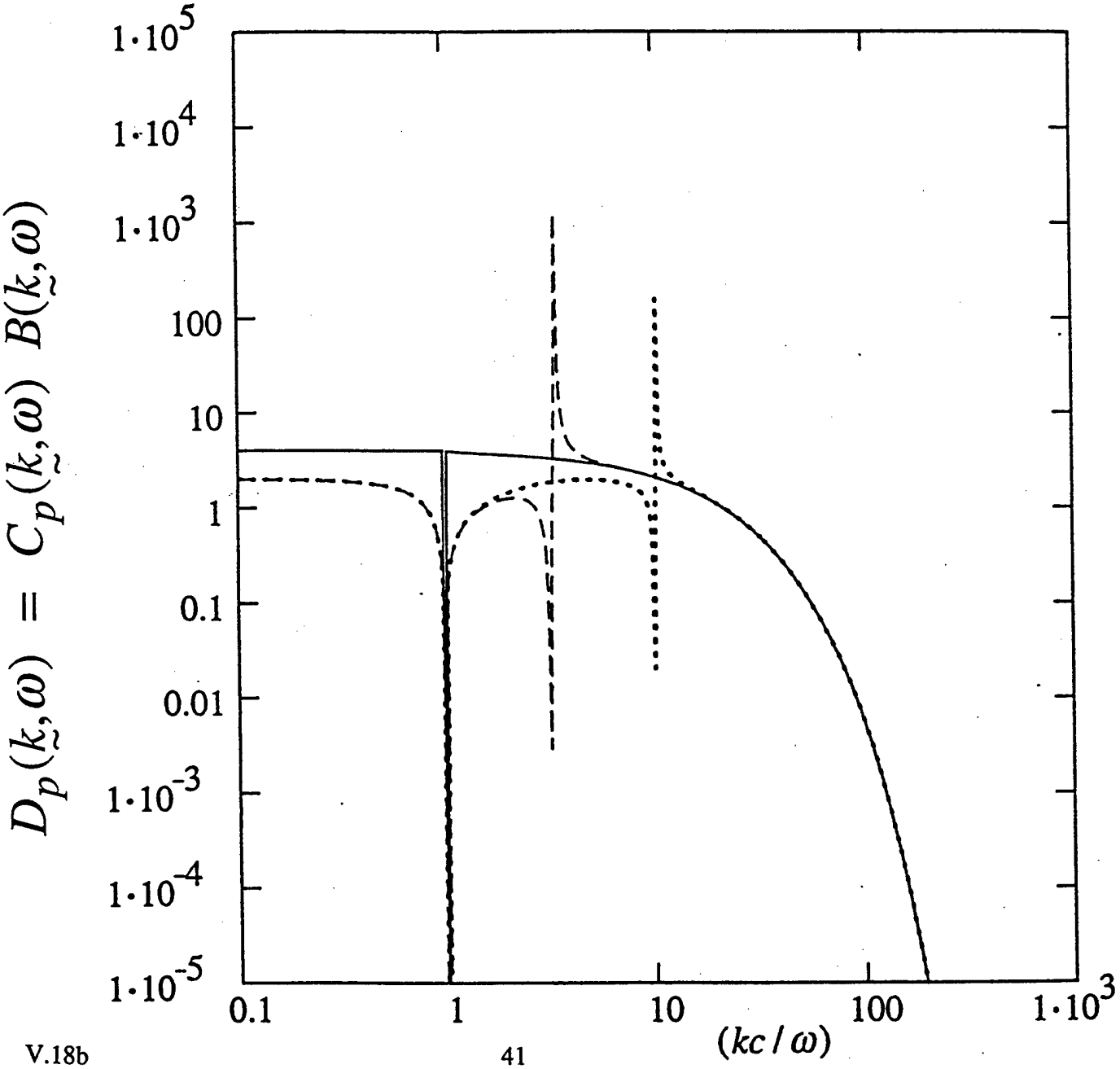

Viewgraph 19

Equating $A_p(\underset{\sim}{k}_s|\underset{\sim}{k},\omega)$, $A_v(\underset{\sim}{k}_s|\underset{\sim}{k},\omega)$ and $[A_v^o(\underset{\sim}{k}_s|\underset{\sim}{k},\omega)/(\rho c)^2]$ states that the absolute value of the sensitivity in the two arrays to a normal incidence are rendered equal and that, hence, the steering filtering efficiencies are rendered identical. In this calibration the boundaries are assumed to yield the same values for the passive filtering efficiency for that normal incidence. It remains to examine the passive filtering efficiency $D_v(\underset{\sim}{k},\omega)$ for the velocity array.

Thus, once $D_p(\underset{\sim}{k},\omega)$ and $D_v(\underset{\sim}{k},\omega)$ are determined a comparison of the outputs of the two arrays can be ascertained.

Filtering Efficiency for a Velocity Array

$$O_v(\underset{\sim}{k}_s,\omega) = \int d\underset{\sim}{k}\ J_v^o(\underset{\sim}{k}_s \mid \underset{\sim}{k},\omega)\ \Phi_v(\underset{\sim}{k},\omega) \ ;$$

$$J_v^o(\underset{\sim}{k}_s \mid \underset{\sim}{k},\omega) = A_v^o(\underset{\sim}{k}_s \mid \underset{\sim}{k},\omega) D_v^o(\underset{\sim}{k}_s \mid \underset{\sim}{k},\omega) \ ;$$

where (ρc) is the characteristic impedance of the fluid and $\Phi_v(\underset{\sim}{k},\omega) = \mid 1-(kc/\omega)^2 \mid (\rho c)^{-2}\Phi_p(\underset{\sim}{k},\omega)$. Then

$$O_v(\underset{\sim}{k}_s,\omega) = \int d\underset{\sim}{k}\ J_v(\underset{\sim}{k}_s \mid \underset{\sim}{k},\omega)\ \Phi_p(\underset{\sim}{k},\omega) \ ;$$

$$J_v(\underset{\sim}{k}_s \mid \underset{\sim}{k},\omega) = A_v(\underset{\sim}{k}_s \mid \underset{\sim}{k},\omega)\ D_v(\underset{\sim}{k},\omega) \ ,$$

where

$$A_v(\underset{\sim}{k}_s \mid \underset{\sim}{k},\omega) = A_v^o(\underset{\sim}{k}_s \mid \underset{\sim}{k},\omega/(\rho c)^2 \ ;$$

$$D_v(\underset{\sim}{k},\omega) = D_v^o(\underset{\sim}{k},\omega)E_p^v(\underset{\sim}{k},\omega); \quad E_p^v(\underset{\sim}{k},\omega) = \mid 1-(kc/\omega)^2 \mid .$$

Equate

$$A_p(\underset{\sim}{k}_s \mid \underset{\sim}{k},\omega) \equiv A_v(\underset{\sim}{k}_s \mid \underset{\sim}{k},\omega) = [A_v^o(\underset{\sim}{k}_s \mid \underset{\sim}{k},\omega)/(\rho c)^2] \ .$$

Viewgraph 20

[c.f., Viewgraph 15.]

Passive Filtering Efficiency for a Velocity Array

The incident velocity $V(\underset{\sim}{k},\omega)$ on the boundary is presented as

$$V_b(\underset{\sim}{k},\omega) = V(\underset{\sim}{k},\omega)[1+R_v(\underset{\sim}{k},\omega)];\ \ R_v(\underset{\sim}{k},\omega) = -R_p(\underset{\sim}{k},\omega)$$

where $R_v(\underset{\sim}{k},\omega)$ is the reflection coefficient of the boundary

$$R_v(\underset{\sim}{k},\omega) = [Z_w(\underset{\sim}{k},\omega) - Z_b(\underset{\sim}{k},\omega)][Z_w(\underset{\sim}{k},\omega) + Z_b(\underset{\sim}{k},\omega)]^{-1},$$

and again, $Z_b(\underset{\sim}{k},\omega)$ is the mechanical surface impedance of the boundary, which for the velocity array is selected to be compliant; e.g.,

$$Z_b(\underset{\sim}{k},\omega) \ = \ (K/i\omega) \ \ ; \ \ K \ = \ K_o(1+i\eta_o) \ \ ,$$

The factor $[1+R_v(\underset{\sim}{k},\omega)]$ is the conditioning compliance filtering function; the filtering efficiency $C_v(\underset{\sim}{k},\omega)$ of the conditioning compliance is given by

$$C_v(\underset{\sim}{k},\omega) \ = \ |1-R_p(\underset{\sim}{k},\omega)|^2$$

$$= \ 4\,|Z_w(\underset{\sim}{k},\omega)|^2 \ \ |Z_b(\underset{\sim}{k},\omega) \ + \ Z_w(\underset{\sim}{k},\omega)|^{-2} \ \ .$$

V.20

Viewgraph 21a

An ideal compliance is one that renders $|Z_w(\underset{\sim}{k},\omega)| >> |Z_c(\underset{\sim}{k},\omega)|$ throughout the relevant spectral range of concern. In this case the fluid-surface impedance is the dominant impedance on the boundary. This condition is predicated on the auxiliary condition that demands that $|Z_p(\underset{\sim}{k},\omega)| >> |Z_c(\underset{\sim}{k},\omega)|$ so that the mechanical surface impedance of the boundary is dominated by the compliance of the layer. [cf. Viewgraphs 3 and 4.] The ideal conditioning compliance is one for which

$$[K_o/(\omega\rho c)] = \varepsilon_o << 1 \; ; \quad \varepsilon_o \; (K_o/\omega_o\rho c) \; ; \quad \omega = \omega_o \; ,$$

where (ω_o) is the resonance frequency of the surface stiffness of the compliant layer and the surface mass of the fluid. The inverse fluid loading parameter (ε_o) is the inverse fluid loading factor at resonance. The condition for this resonance is given by

$$(kc/\omega)_o^2 \quad = \quad 1+(\varepsilon_o)^{-2} \quad ; \quad \omega = \omega_o \; ,$$

where the subscript (o) indicated quantities at resonance. In order to maintain $C_v(\underset{\sim}{k},\omega)$ close to the value of (4) in the relevant range

$$\varepsilon_o << 10^{-2} \; ,$$

must be obeyed, which confirms the ideal conditioning compliance requirement. The condition is commensurate with a "pressure release boundary". Thus the ideal conditioning compliance is that of a pressure release boundary. [cf. Viewgraph 16a.] For a pressure release boundary $C_v(\underset{\sim}{k},\omega) \simeq 4$ in the relevant range; i.e., a velocity doubling at the boundary.

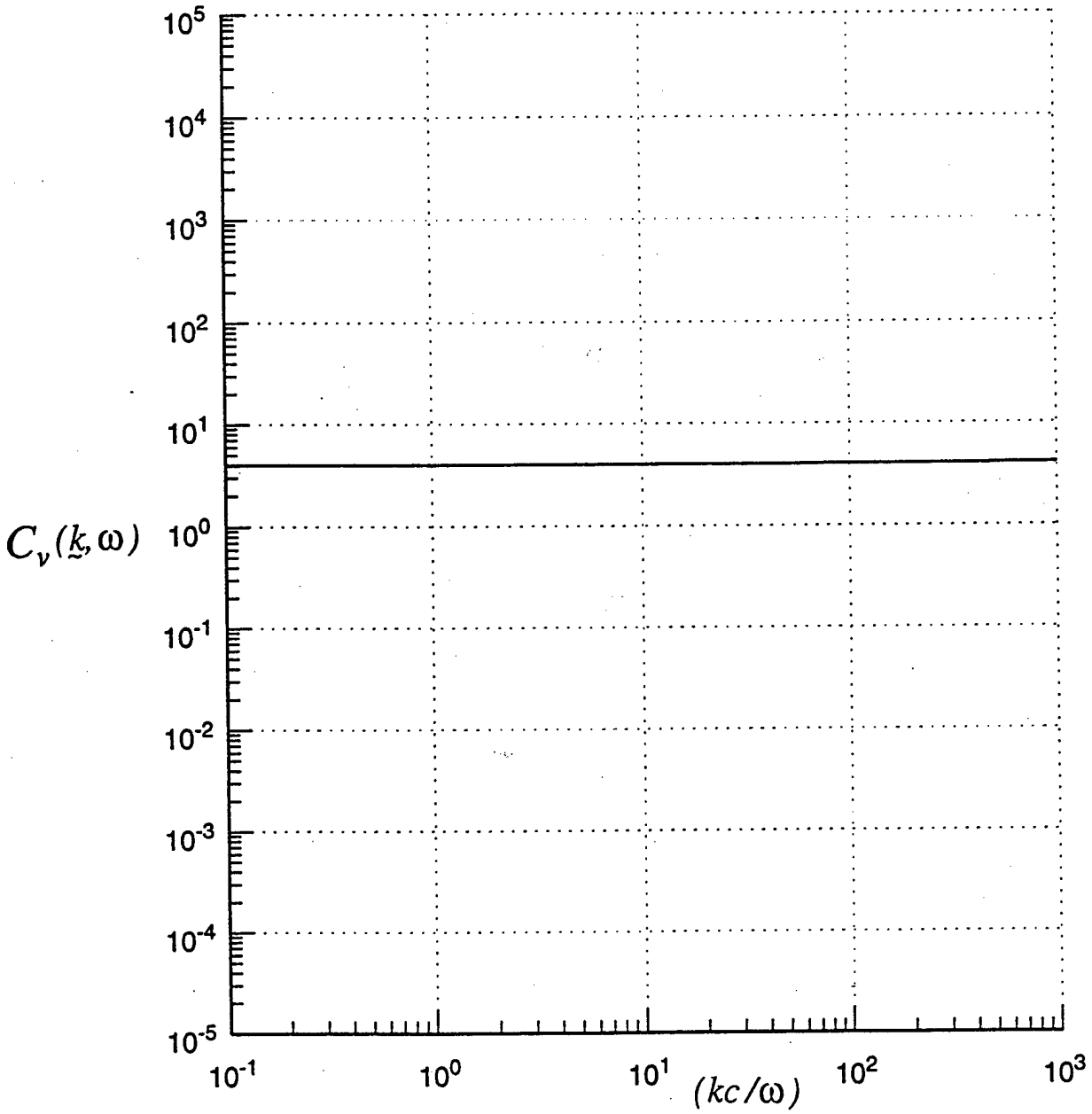
$C_v(\underset{\sim}{k},\omega)$
10^5
10^4
10^3
10^2
10^1
10^0
10^{-1}
10^{-2}
10^{-3}
10^{-4}
10^{-5}
10^{-1}
10^0
10^1
10^2
10^3
(kc/ω)

Viewgraph 21b

What is the situation if the resonance is allowed to occur in the range just above the sonic range; i.e., if (ε_o) is assumed small compared with unity but not negligible. The conditions are

$$(kc/\omega)_o^2 = 1+(\varepsilon_o)^{-2} \;\; ; \;\; \varepsilon_o = 10^{-1} << 1 \;\; ; \;\; (kc/\omega)_o^2 = 1+10^2 \;\; ; \;\; \omega = \omega_o \;\; ,$$

so that $(kc/\omega)_o \simeq 10$. The resonance and its influence on the filtering efficiency $C_v(\underset{\sim}{k},\omega)$ of the conditioning compliance is illustrated on the viewgraph. Of particular interest is the post resonance nature of $C_v(\underset{\sim}{k},\omega)$. The values of $C_v(\underset{\sim}{k},\omega)$ are drastically diminished with increase in (kc/ω) past the resonance location at $(kc/\omega)_o$. The diminishing is of benefit to the array; the decrease occurs in the subsonic range where only noise components reside. [cf. Viewgraph 17 for comparison with the filtering efficiency of a blanket.] There is, however, a penalty associated with this benefit; at and in the vicinity of the resonance there is an increase in $C_v(\underset{\sim}{k},\omega)$. Whether on balance it is beneficial or detrimental to introduce a resonance depends critically on the distribution of components of the noise in the subsonic range. Can (ε_o) be further increased? Well, (ε_o) much beyond unity will interfere with the maintenance of $C_v(\underset{\sim}{k},\omega)$ at the value of (4) in the supersonic range; not a good design procedure. The situation for $\varepsilon_o = 1$ is also illustrated on the viewgraph. It is observed that some erosion in the value of $C_v(\underset{\sim}{k},\omega)$ occurs in the supersonic range. A decrease in $C_v(\underset{\sim}{k},\omega)$ in this supersonic range diminishes the sensitivity of the array to components in the signal, not a good design procedure either. However, when $\varepsilon_o = 1$, the diminishing of $C_v(\underset{\sim}{k},\omega)$ in the subsonic range, commences earlier and the range occupied by the resonance is decreased. Again, whether rendering $\varepsilon_o = 1$ is more beneficial than detrimental is matter to be investigated.

The filtering efficiency $C_v(\underset{\sim}{k},\omega)$ of a compliantly conditioned boundary,

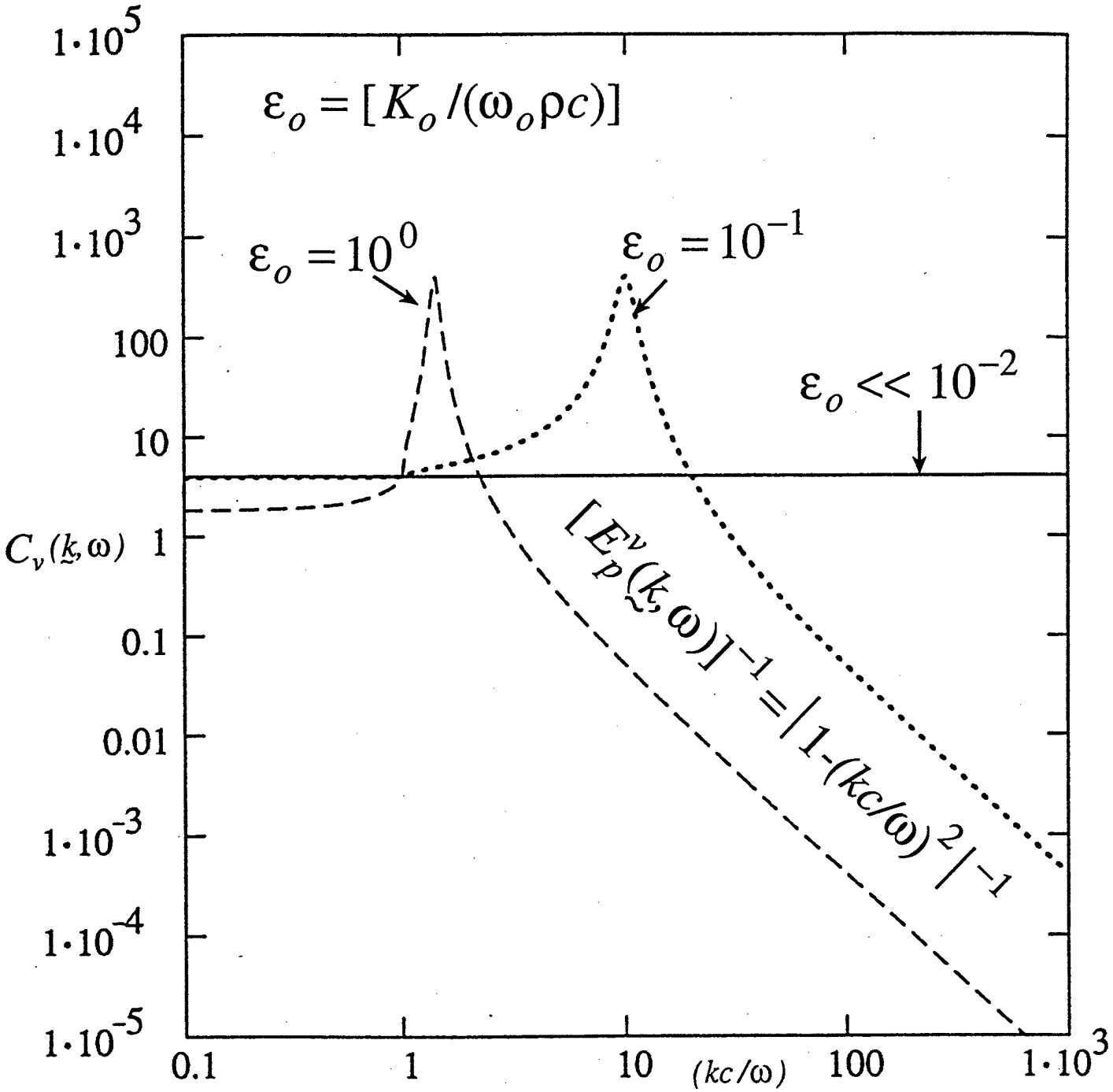

Resonance of the surface stiffness of compliant layer and surface mass of fluid.

Viewgraph 22

Inherent to the velocity array is the conversion filtering efficiency $E_p^v(\underset{\sim}{k},\omega)$. This factor in the filtering efficiency of the velocity array is dependent merely on the parameter (kc/ω); it is assumed to be independent of any of the material properties of the array. The conversion filtering efficiency $E_p^v(\underset{\sim}{k},\omega)$ is depicted as a function of (kc/ω) on the viewgraph. In the supersonic range super-directivity effects are exhibited, culminating with the plunge to zero at the sonic location. A recovery, accompanied by a steep increase, at the rate of $(kc/\omega)^2$, is observed, as (kc/ω) is further increased into the subsonic range. This monopole-to-dipole, dipole-to-quadrapole, etc., behavior, is typical of pressure-to-velocity arrays. How detrimental is the presence of the conversion filtering efficiency $E_p^v(\underset{\sim}{k},\omega)$ of the velocity array to its utilization? The super-directivity in the supersonic range may, in certain situations, be taken advantage of to enhance the filtering efficiency of the array in this range. The higher and higher values of the conversion filtering efficiency, at the higher and higher subsonic ranges, cannot be but detrimental to the overall filtering efficiency of the array. This detrimental affect is especially true if the noise components that reside in these higher and higher subsonic ranges are significant even for the pressure array in which the conversion filtering efficiency is absent.

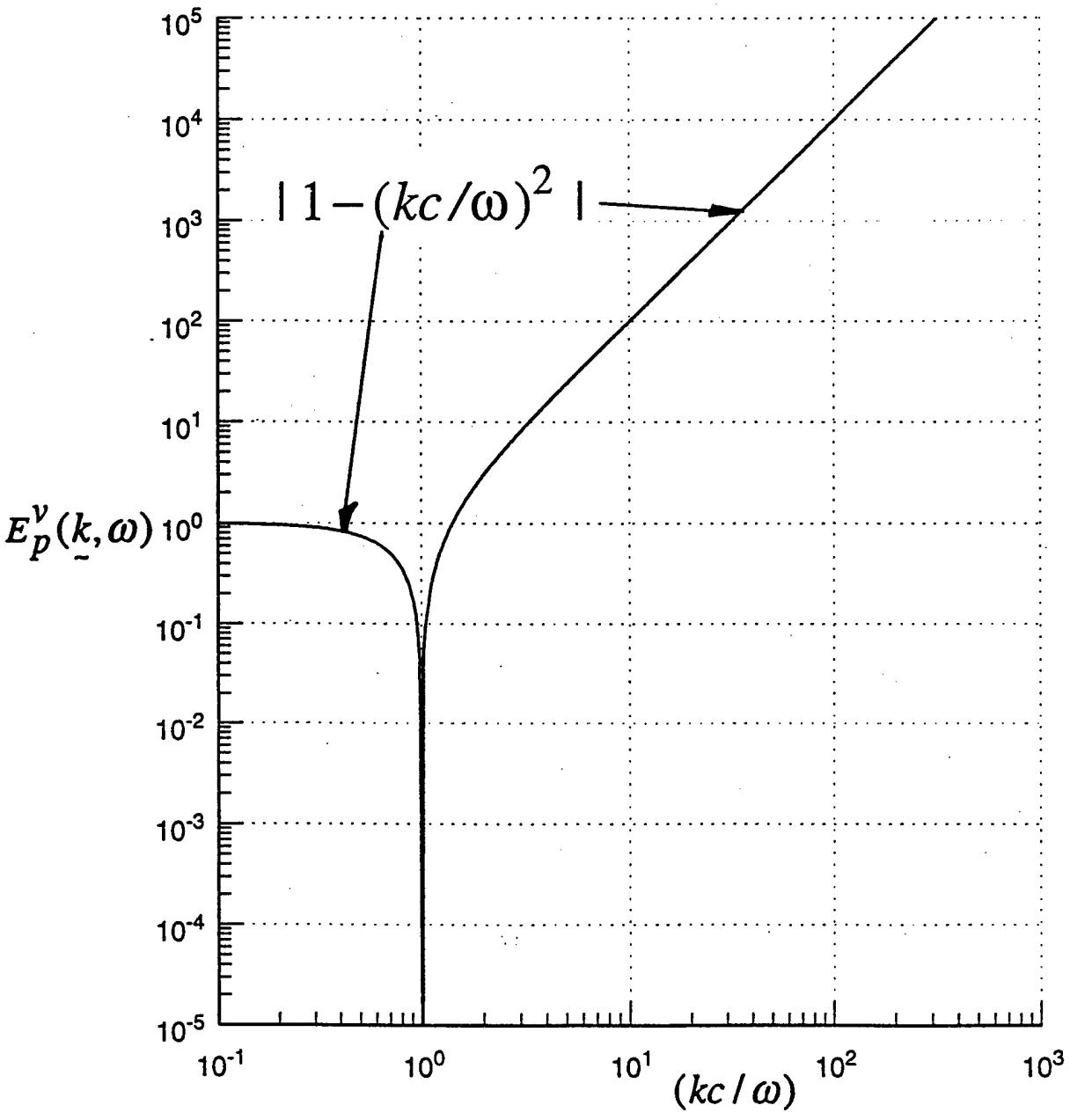
$|1-(kc/\omega)^2|$
$E_p^v(\underset{\sim}{k},\omega)$
10^5
10^4
10^3
10^2
10^1
10^0
10^{-1}
10^{-2}
10^{-3}
10^{-4}
10^{-5}
10^{-1}
10^0
10^1
10^2
10^3
(kc/ω)

Viewgraph 23a

The ideal passive filtering efficiency of the boundary of a velocity array is given by

$$D_{1v}(\underset{\sim}{k},\omega) \;=\; C_v(\underset{\sim}{k},\omega)E_p^v(\underset{\sim}{k},\omega) \quad ,$$

with $C_v(\underset{\sim}{k},\omega)$ and $E_p^v(\underset{\sim}{k},\omega)$ as shown in Viewgraphs 21a and 22, respectively. In this viewgraph the ideal passive filtering efficiency of the boundary of a velocity array is presented as a function of (kc/ω). The detrimental effects of the conversion filtering efficiency $E_p^v(\underset{\sim}{k},\omega)$ are clearly demonstrated and are driven home by comparing this viewgraph with that presented in Viewgraph 16a. The detriment is largely in the higher and higher subsonic range.

The ideal filtering efficiency $D_{1v}(\underset{\sim}{k},\omega) = \{[C_v(\underset{\sim}{k},\omega)E_p^v(\underset{\sim}{k},\omega)]\}$ of an ideally, but compliantly conditioned boundary (a pressure release boundary) taking account of the conversion filtering efficiency.

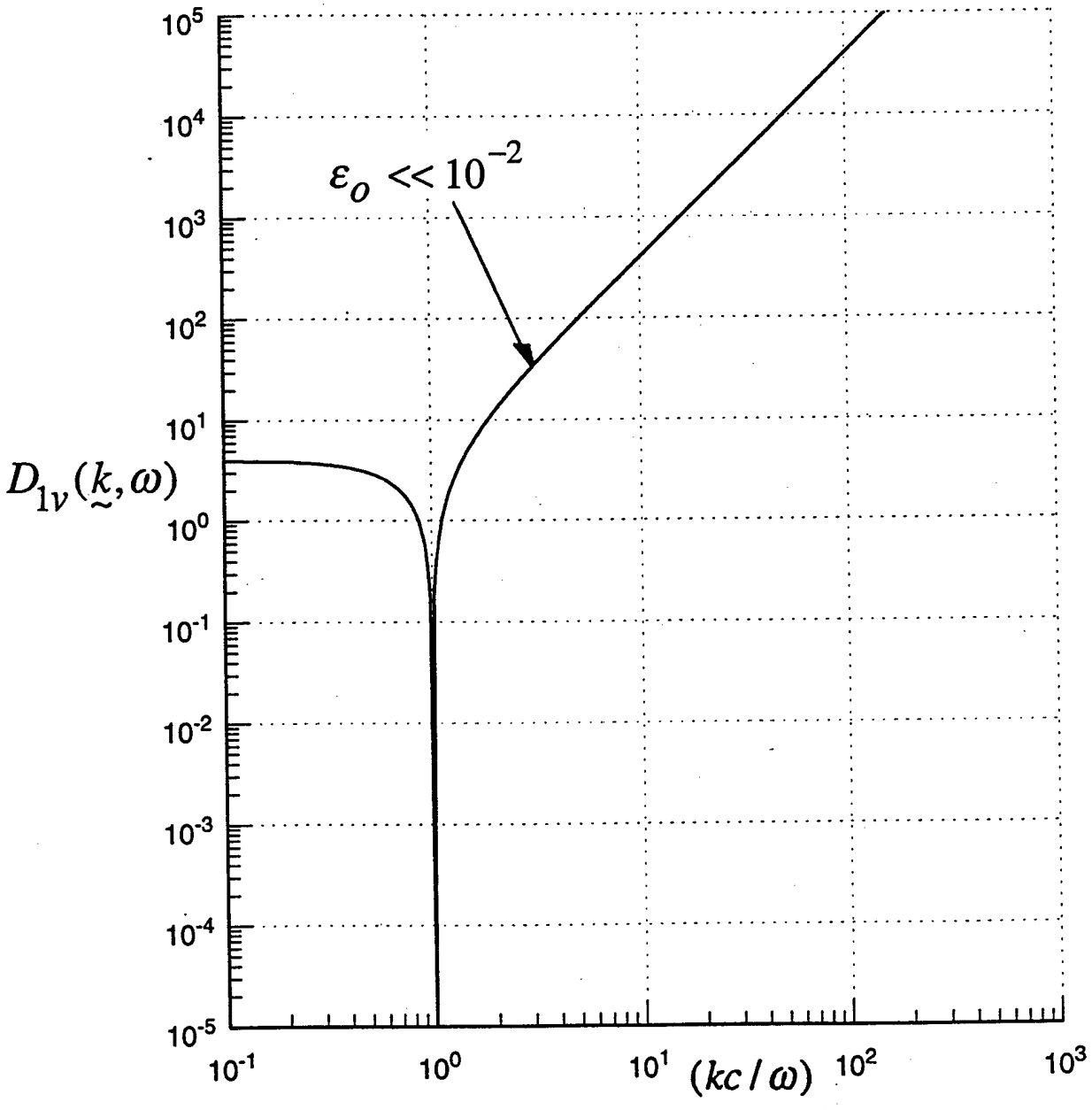

Viewgraph 23b

One recalls that the resonance in the conditioning compliance benefited the filtering efficiency of the boundary in the subsonic range exactly where the detrimental affects of the conversion filtering efficiency occur. May one hope that this resonance could mitigate these detrimental affects? Indeed, beyond the resonance at $(kc/\omega)_o$, the rise in one corresponds to the fall in the other. The viewgraph shows the extent of this mitigation using Viewgraphs 21b and 22. Clearly the "rise and fall" match each other, but only in the range beyond $(kc/\omega)_o$. Also, the increase in $D_{1v}(\underset{\sim}{k},\omega)$, at and in the vicinity of the location of the resonance, is clearly discernible. Of course except for this peak in $D_{1v}(\underset{\sim}{k},\omega)$ with $\varepsilon_o = 1$, it favorably competes with $C_p(\underset{\sim}{k},\omega)$ presented in Viewgraph 16b with $\varepsilon_c = 10^{-1}$ and $(\omega_c/\omega) = 10$. One finds that the devastating affects introduced into the velocity array by $E_p^v(\underset{\sim}{k},\omega)$ can be largely mitigated by rendering the boundary with a conditioning compliance for which $\varepsilon_o = 1$. A narrow region in (kc/ω), about $(kc/\omega)_o$, remains, nonetheless, troublesome. How troublesome is this peak in the passive-filtering efficiency is yet to be determined; e.g., if there are noise components that reside in this narrow region, a troublesome situation may exist. In the absence of such noise components, the filtering efficiency of the boundaries in the two cases; a pressure array and a velocity array, may be largely on par.

The filtering efficiency $D_{1v}(\underset{\sim}{k},\omega) = \{[C_v(\underset{\sim}{k},\omega)E_p^v(\underset{\sim}{k},\omega)]\}$ of a compliantly conditioned boundary taking account of the conversion filtering efficiency.

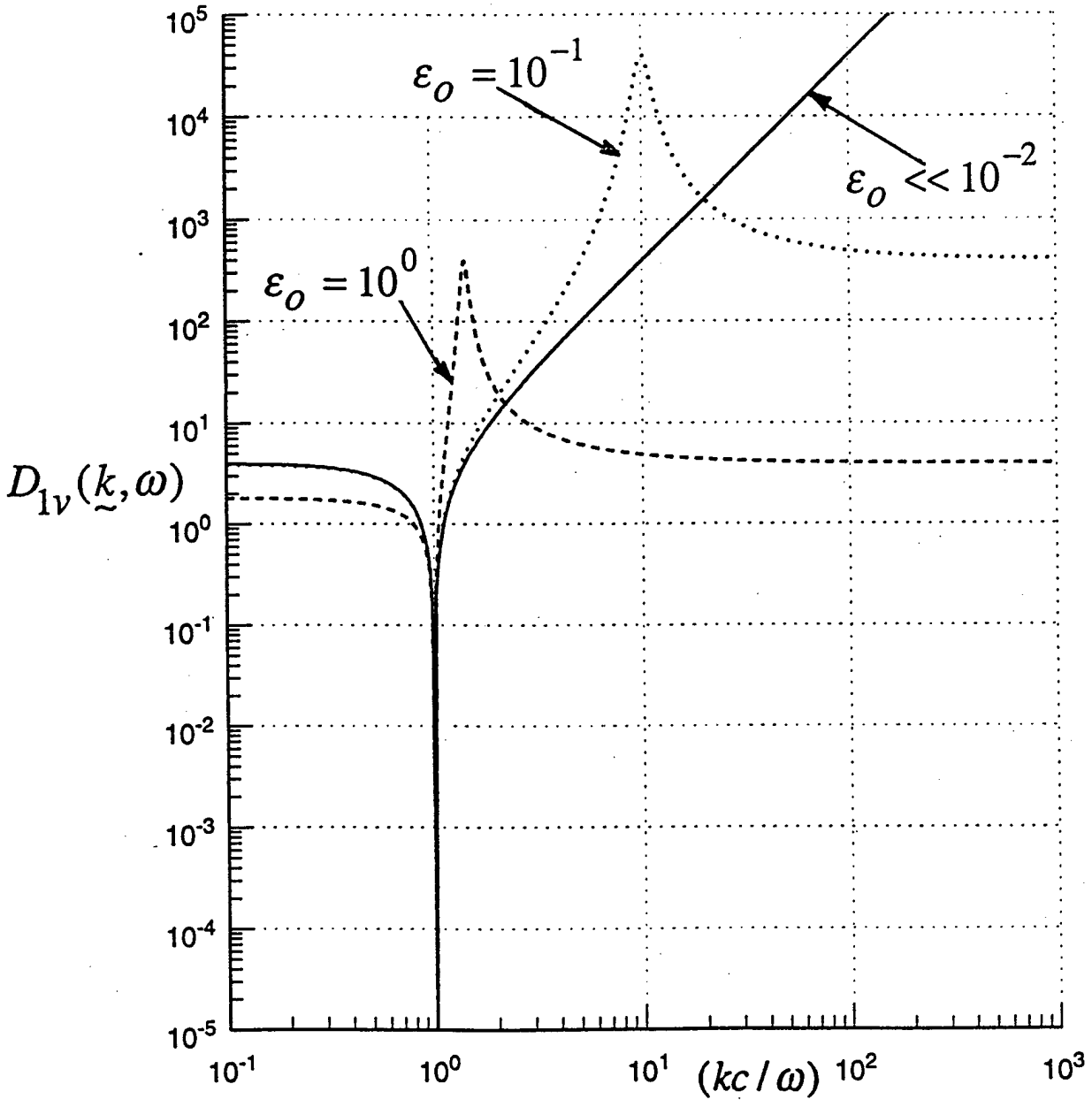

Viewgraph 24

The blanket may also be introduced onto the boundary in which the velocity array is flush mounted. The filtering efficiency of the blanket on a velocity array is assumed to be that on a pressure array. The latter is depicted in Viewgraph 17. The standard blanket is that corresponding to a thickness (b) given by $(b\omega/c) = (1/30)$. Cladding the velocity array with a blanket yields a passive filtering efficiency $D_v(\underset{\sim}{k},\omega)$ for the velocity array

$$D_v(\underset{\sim}{k},\omega) \;=\; D_{1v}(\underset{\sim}{k},\omega)B(\underset{\sim}{k},\omega) \;;\; D_{1v}(\underset{\sim}{k},\omega) \;=\; C_v(\underset{\sim}{k},\omega)\; E_p^v(\underset{\sim}{k},\omega)\;.$$

The placing of a standard blanket on a velocity array, for which $D_{1v}(\underset{\sim}{k},\omega)$ is as depicted in Viewgraph 23b, yields a passive filtering efficiency $D_v(\underset{\sim}{k},\omega)$ as depicted in the viewgraph. The benefit of a blanket to the passive filtering efficiency in the subsonic range is clearly demonstrated in the viewgraph. [cf. Viewgraph 18b.] Of particular interest is that the blanket wins over the severe filtering deficiency in the higher subsonic range. This severe filtering deficiency is introduced by the conversion filtering efficiency $E_p^v(\underset{\sim}{k},\omega)$ that is inherent to the velocity array. [Exponential versus quadratic dependence.] Since the resonance in $C_v(\underset{\sim}{k},\omega)$, with $\varepsilon_o = 1$, is close to the sonic location, the blanket is hardly effective with respect to the resonance peak in the passive filtering efficiency.

The passive filtering efficiency

$D_v(\underset{\sim}{k},\omega) = \{[C_v(\underset{\sim}{k},\omega)E_p^v(\underset{\sim}{k},\omega)\,B(\underset{\sim}{k},\omega)]\}$ of a blanketed compliantly conditioned boundary taking account of the conversion filtering efficiency.

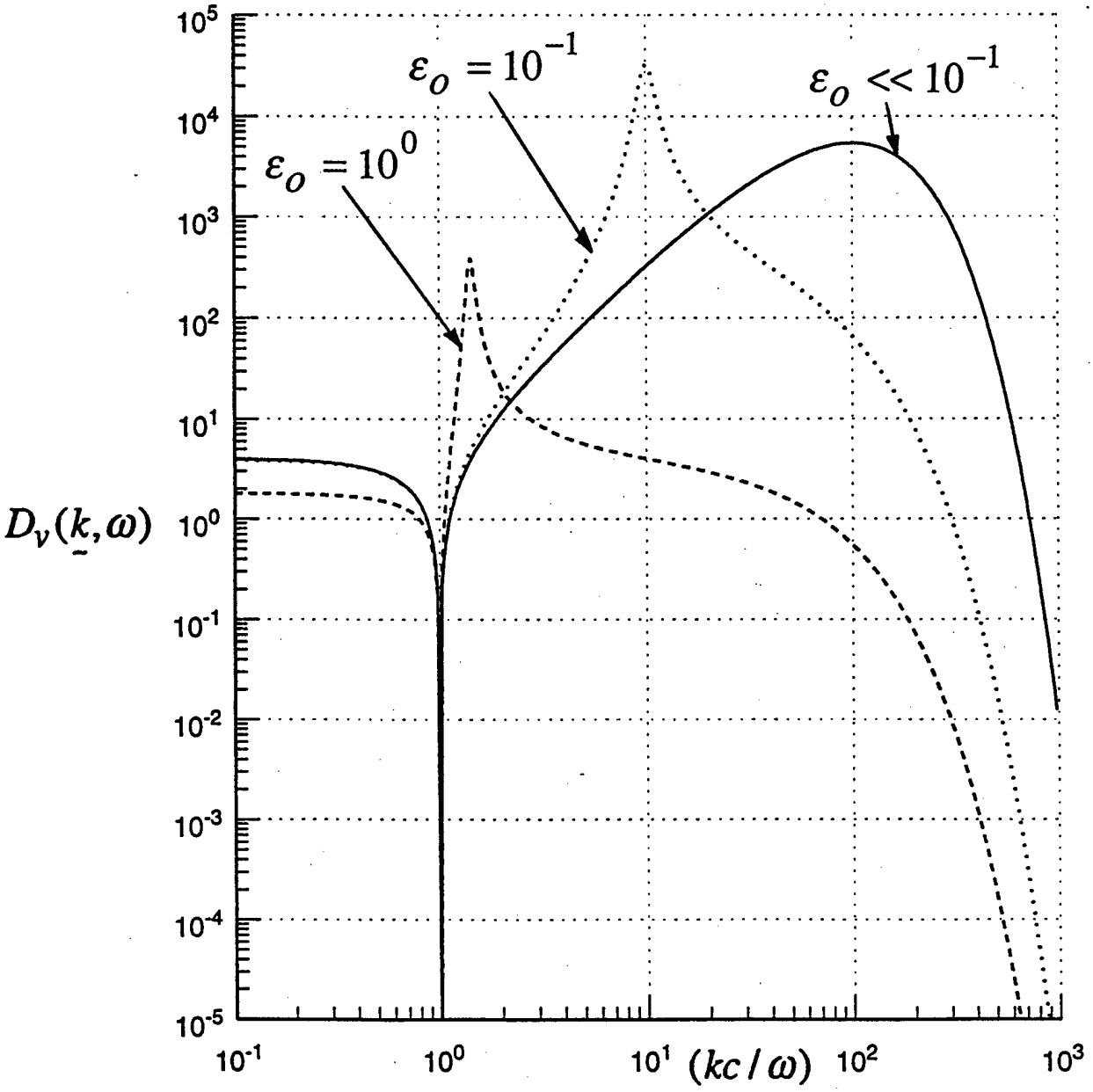

Viewgraph 25

The equivalent factor $T_p^v(\underset{\sim}{k},\omega)$ relates the noise spectral density that a velocity array perceives were its combined filtering efficiency adjusted to be that of a corresponding pressure array. Since the steered filtering efficiencies of the two array types are properly calibrated and since the signal spectral density is confined to the supersonic range, the equivalent factor also relates the signal spectral density that a velocity array perceives were its combined filtering efficiency adjusted to be that of a corresponding pressure array.

$$O_{pS}(\underset{\sim}{k}_s,\omega) = \int d\underset{\sim}{k} J_p(\underset{\sim}{k}_s|\underset{\sim}{k},\omega)\ U[1-(kc/\omega)]\ \Phi_{pS}(\underset{\sim}{k},\omega) \quad ;$$

$$O_{vS}(\underset{\sim}{k}_s,\omega) = \int d\underset{\sim}{k} J_p(\underset{\sim}{k}_s|\underset{\sim}{k},\omega)\ U[1-(kc/\omega)]\ \Phi_{vS}(\underset{\sim}{k},\omega) \quad ;$$

$$[\Phi_{vS}(\underset{\sim}{k}_s,\omega) = T_p^v(\underset{\sim}{k},\omega)\Phi_{pS}(\underset{\sim}{k},\omega)]\ U[1-(kc/\omega)] \quad .$$

An example for the signal spectral density may be cast in the form

$$\Phi_{pS}(\underset{\sim}{k}_s,\omega) = \Phi_S(\underset{\sim}{k}_s,\omega)\ \delta(k_x-k_{sx})\ \delta(k_y-k_{sy}) \quad .$$

Equivalent Factor $T_p^v(\underset{\sim}{k},\omega)$ between the pressure and

velocity arrays

$$O_{pN}(\underset{\sim}{k}_s,\omega) = \int d\underset{\sim}{k}\ J_p(\underset{\sim}{k}_s \mid \underset{\sim}{k},\omega)\ \Phi_{pN}(\underset{\sim}{k},\omega)\ ;$$

$$O_{vN}(\underset{\sim}{k}_s,\omega) = \int d\underset{\sim}{k}\ J_p(\underset{\sim}{k}_s \mid \underset{\sim}{k},\omega)\ \Phi_{vN}(\underset{\sim}{k},\omega)\ ,$$

where

$$J_p(\underset{\sim}{k}_s \mid \underset{\sim}{k},\omega) = A_p(\underset{\sim}{k}_s \mid \underset{\sim}{k},\omega)\ D_p(\underset{\sim}{k},\omega)\ ;$$

$$\Phi_{vN}(\underset{\sim}{k},\omega) = T_p^v(\underset{\sim}{k},\omega)\ \Phi_{pN}(\underset{\sim}{k},\omega)\ ;$$

$$T_p^v(\underset{\sim}{k},\omega) = [D_{1v}(\underset{\sim}{k},\omega)/C_p(\underset{\sim}{k},\omega)]\ .$$

Viewgraph 26

The equivalent factor $T_p^v(\underline{k},\omega)$ cursorily and primitively compares the effectiveness of the filtering efficiency of a velocity array and the corresponding effectiveness of the filtering efficiency of a pressure array. Where $T_p^v(\underline{k},\omega)$ is less than unity, the pressure array is the less effective and where $T_p^v(\underline{k},\omega)$ exceeds unity, the pressure array is the more effective. In the case of the ideal conditioning of both, the pressure and velocity arrays, the pressure array is deficient in the supersonic range as compared to the velocity array. This relative deficiency is due to the super-directivity in the filtering efficiency of the velocity array. However, the relative deficiency in this range affects the signal as well as the noise. Nonetheless, situations may arise in which this super-directivity in the velocity array may be advantaged. On the other hand, in the subsonic range the filtering efficiency of the pressure array is superior to that of the corresponding velocity array. This superiority is higher the higher the subsonic range is. Thus, according to the viewgraph, if the pressure array has a marginal signal-to-noise ratio because of a noise spectral density that largely resides in the subsonic range, the corresponding velocity array has a signal-to-noise ratio that is hopeless. Problems: (+) Super-directivity may be put to a combined filtering advantage. (-) Ideal conditioning compliance implies "a pressure release boundary." Such a boundary is hardly suitable for underwater use.

Equivalent Factor $T_p^{\upsilon}\ (\underset{\sim}{k},\omega)$ under ideal conditions on both the pressure and velocity arrays

$[\varepsilon_c << 1 << (\omega_c/\omega)]$ and $[\varepsilon_o << 1]$.

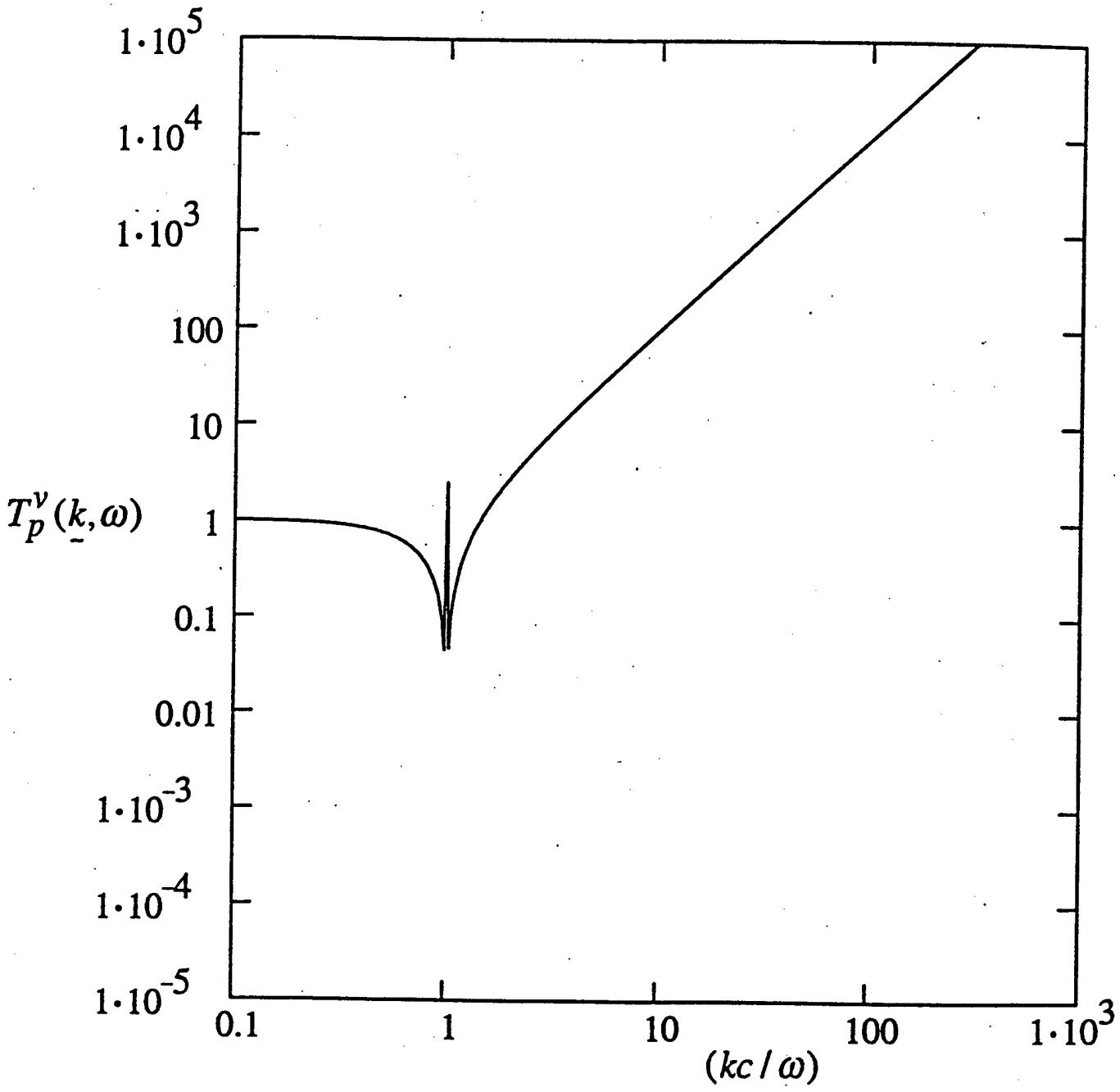

Viewgraph 27

Can a more realistic conditioning of the boundary render the equivalent factor $T_p^v(\underset{\sim}{k},\omega)$ more favorable to a velocity array than the prognosis in Viewgraph 26 indicates? A clue that this may be the case is argued in Viewgraph 23b. In the present viewgraph a situation is depicted in which the conditioning compliance is defined by an inverse fluid loading parameter (ε_o) that is equal to (10^{-1}). An improvement over the equivalent factor $T_p^v(\underset{\sim}{k},\omega)$ depicted in Viewgraph 26 is clearly indicated in the present viewgraph. There is, however, a slight deterioration in a narrow range of (kc/ω) centered about the value of $(kc/\omega)_o = (10)$, where the resonance is located. Moreover, the improvement is largely in the range of (kc/ω) that is above the location of the resonance at $(kc/\omega)_o$. Will reduction in the location of the resonance from $(kc/\omega)_o$ equal to (10) to $(kc/\omega)_o = (\sqrt{2})$ further improve the equivalent factor $T_p^v(\underset{\sim}{k},\omega)$ in favor of the velocity array?

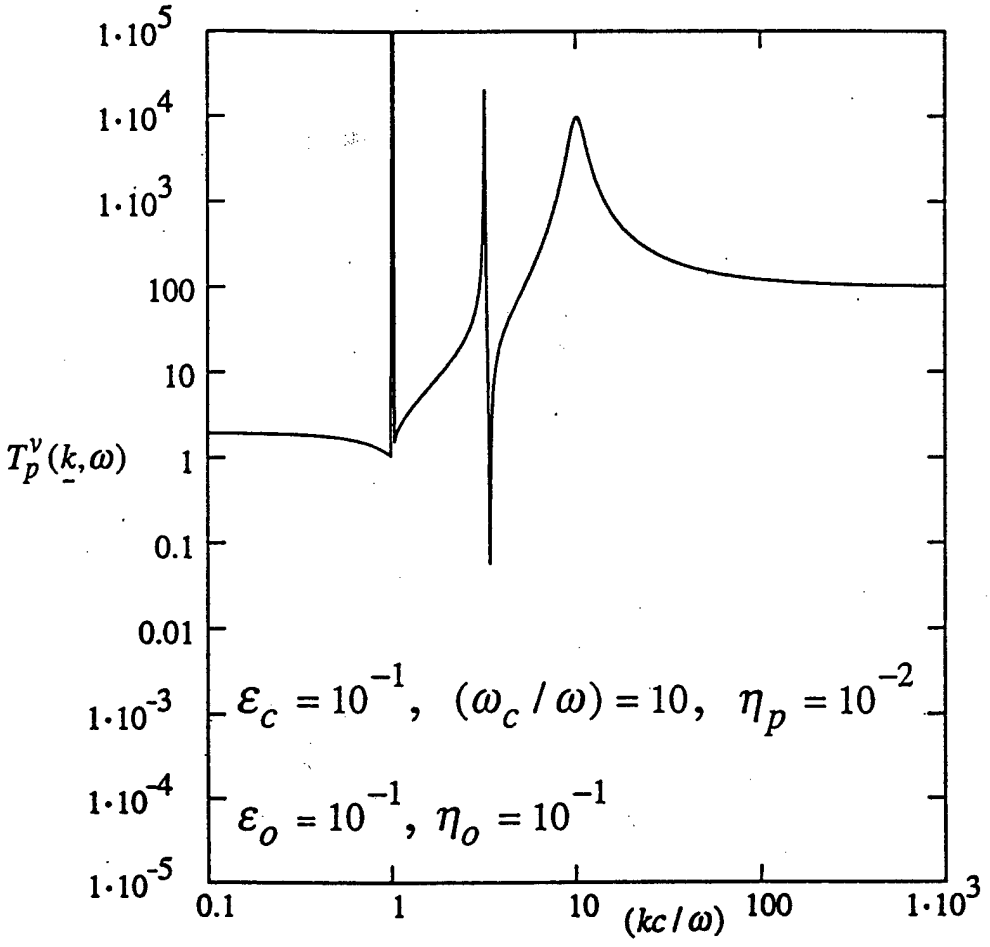
$1\cdot10^5$
$1\cdot10^4$
$1\cdot10^3$
100
10
1
0.1
0.01
$1\cdot10^{-3}$
$1\cdot10^{-4}$
$1\cdot10^{-5}$
$T_p^{\nu}(\underline{k},\omega)$
$\varepsilon_c = 10^{-1}$, $(\omega_c/\omega) = 10$, $\eta_p = 10^{-2}$
$\varepsilon_o = 10^{-1}$, $\eta_o = 10^{-1}$
0.1
1
10
100
$1\cdot10^3$
(kc/ω)

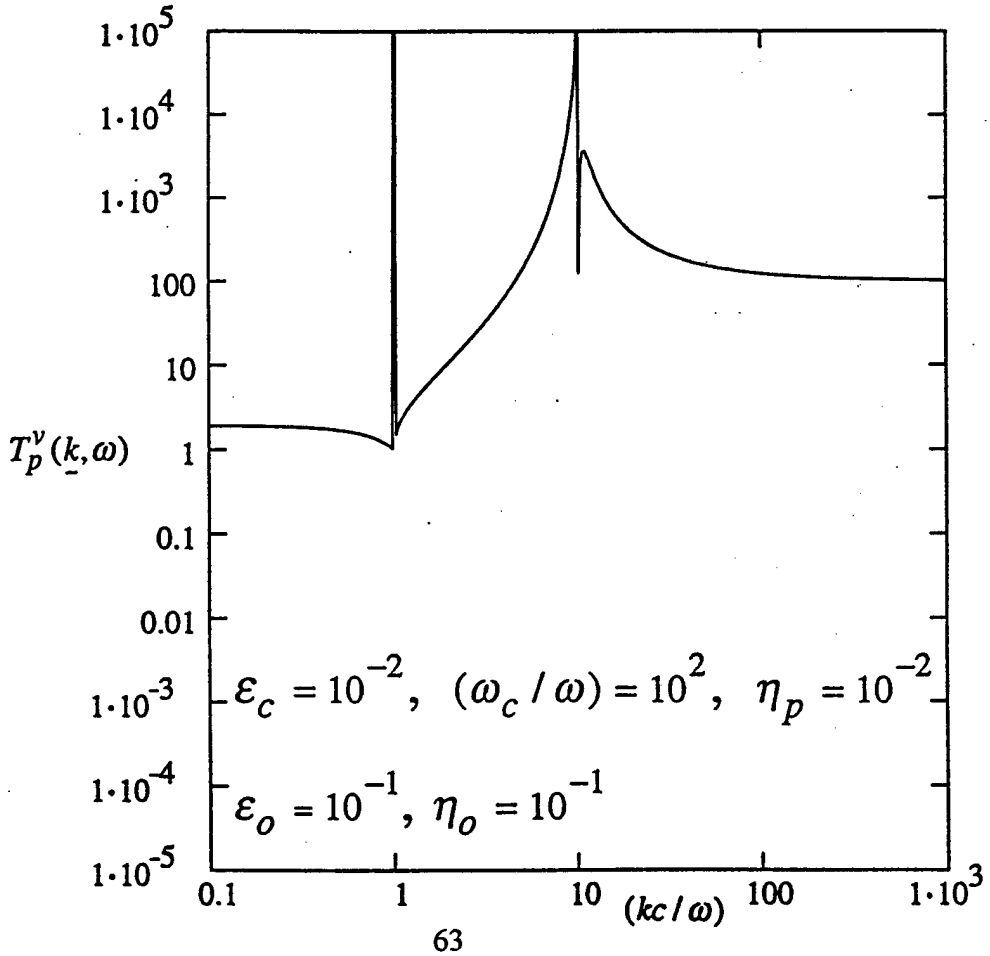
$1\cdot10^5$
$1\cdot10^4$
$1\cdot10^3$
100
10
1
0.1
0.01
$1\cdot10^{-3}$
$1\cdot10^{-4}$
$1\cdot10^{-5}$
$T_p^{\nu}(\underline{k},\omega)$
$\varepsilon_c = 10^{-2}$, $(\omega_c/\omega) = 10^2$, $\eta_p = 10^{-2}$
$\varepsilon_o = 10^{-1}$, $\eta_o = 10^{-1}$
0.1
1
10
100
$1\cdot10^3$
(kc/ω)

Viewgraph 28

In this viewgraph the inverse fluid loading parameter (ε_o) is equal to (10^0). An improvement in the equivalent factor $T_p^v(\underset{\sim}{k},\omega)$ in this viewgraph, over that depicted in Viewgraphs 26 and 27, is clearly indicated. There is, however, a deterioration in a narrow range of (kc/ω) centered about the value of $(\sqrt{2})$, where the resonance value $(kc/\omega)_o$ is located. It is thus concluded that provided noise spectral components sparsely reside at and in the vicinity of this resonance location, the signal-to-noise ratio of a velocity array may not fall far short from that of a pressure array.

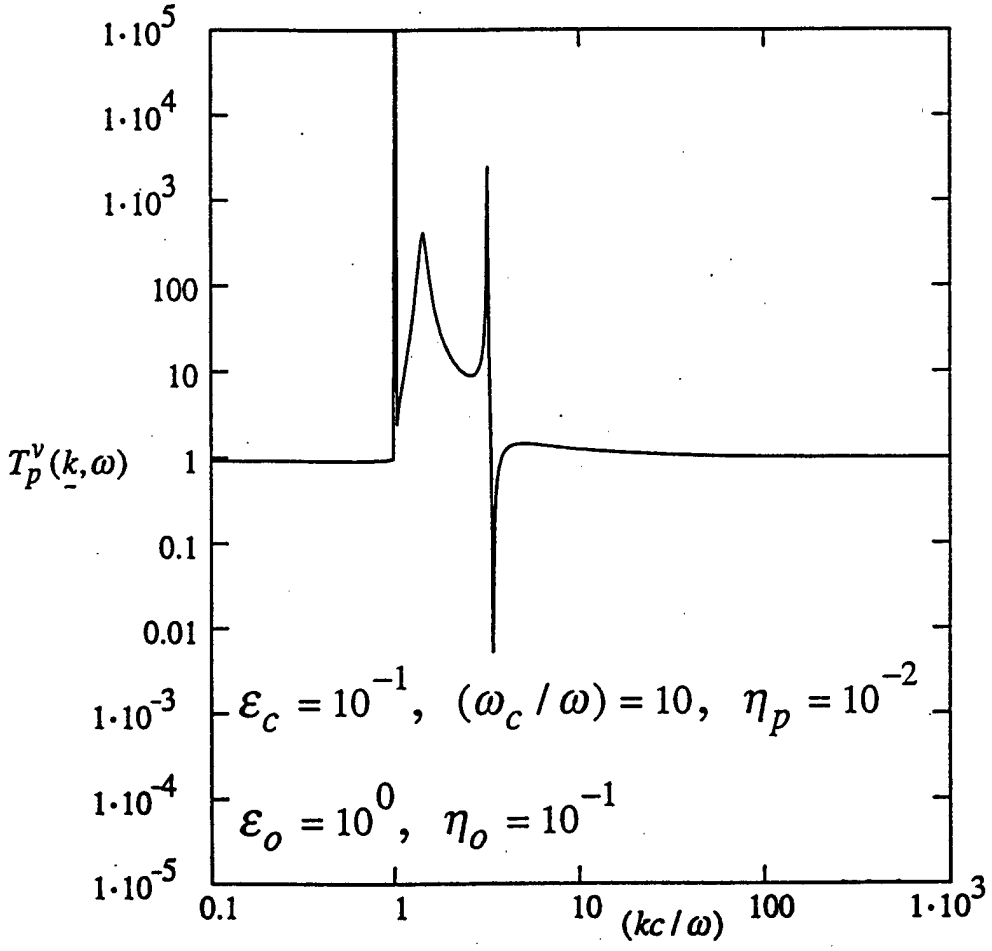
$1\cdot10^5$
$1\cdot10^4$
$1\cdot10^3$
100
10
1
0.1
0.01
$1\cdot10^{-3}$
$1\cdot10^{-4}$
$1\cdot10^{-5}$
$T_p^v(\underline{k},\omega)$
$\varepsilon_c = 10^{-1}$, $(\omega_c/\omega) = 10$, $\eta_p = 10^{-2}$
$\varepsilon_o = 10^0$, $\eta_o = 10^{-1}$
0.1
1
10
100
$1\cdot10^3$
(kc/ω)

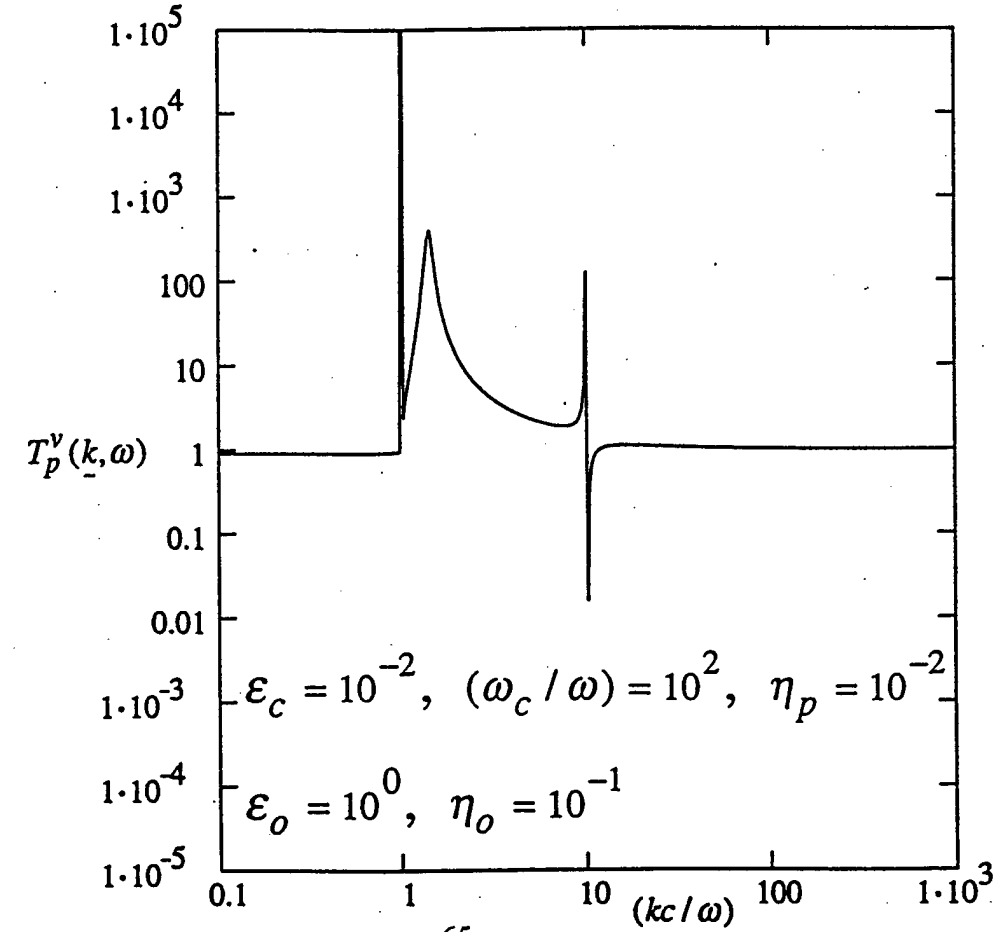
$1\cdot10^5$
$1\cdot10^4$
$1\cdot10^3$
100
10
1
0.1
0.01
$1\cdot10^{-3}$
$1\cdot10^{-4}$
$1\cdot10^{-5}$
$T_p^v(\underline{k},\omega)$
$\varepsilon_c = 10^{-2}$, $(\omega_c/\omega) = 10^2$, $\eta_p = 10^{-2}$
$\varepsilon_o = 10^0$, $\eta_o = 10^{-1}$
0.1
1
10
100
$1\cdot10^3$
(kc/ω)

V.28

Viewgraph 29

A rough sketch of the incident spectral density $\Phi_{TBL}(\underset{\sim}{k},\omega)$ of the pressure in a turbulent boundary layer (TBL) is depicted in this viewgraph. The uncertainty of the low-wavenumber content in $\Phi_{TBL}(\underset{\sim}{k},\omega)$ is emphasized. The narrow dashed line is considered to be the standard incident spectral density to be used subsequently. The convective speed (U_c) of the TBL is assumed, in this report, to be (10^{-2}) of the sound speed (c) in the fluid. The stream-wise and the cross stream-wise spectral densities are depicted in this viewgraph.

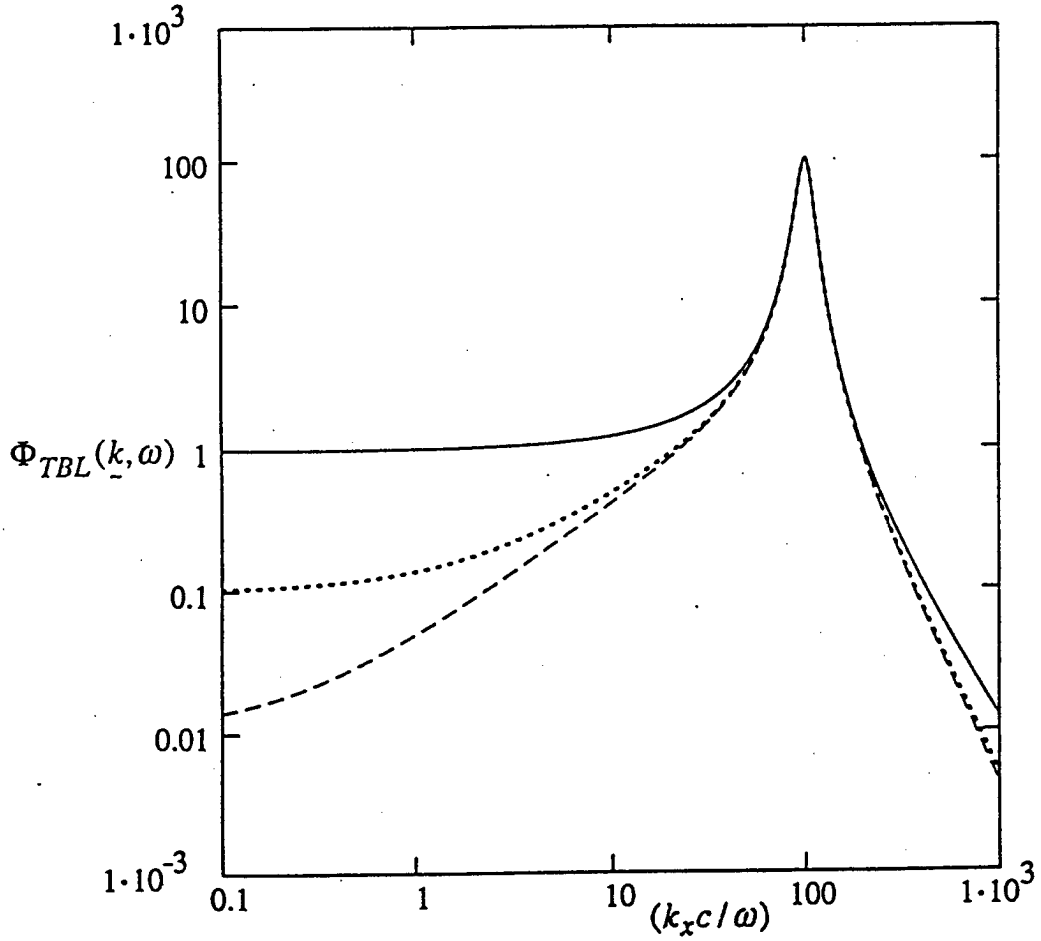
1·10^3
100
10
Φ_TBL(k,ω) 1
0.1
0.01
1·10^-3
0.1
1
10
100
1·10^3
(k_x c / ω)

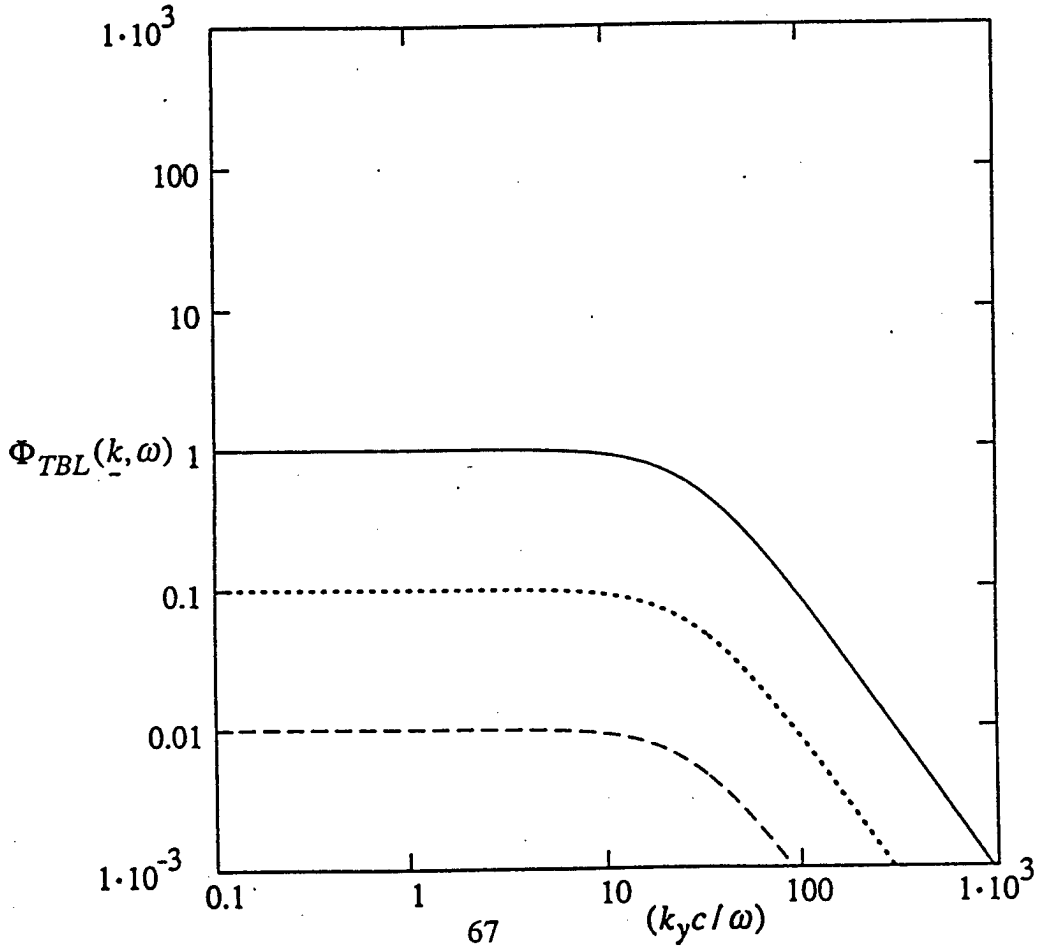
1·10^3
100
10
Φ_TBL(k,ω) 1
0.1
0.01
1·10^-3
0.1
1
10
100
1·10^3
(k_y c / ω)

Viewgraph 30a

The equivalence is given by

$$\Phi_{vN}(\underset{\sim}{k},\omega) = T_p^v(\underset{\sim}{k},\omega)\Phi_{pN}(\underset{\sim}{k},\omega) \quad .$$

If the pressure array perceives $\Phi_{pN}(\underset{\sim}{k},\omega)$ the velocity array perceives equivalently $\Phi_{vN}(\underset{\sim}{k},\omega)$ when the filtering efficiency in the two arrays are rendered equal. [cf. Viewgraph 25.] Clearly, in the stream-wise the equivalent velocity array has to handle much more in the subsonic range and, hence, it will have a poor signal-to-noise compared with the corresponding pressure array were the incident noise largely that in TBL. In this viewgraph the ideal boundaries are employed; i.e., the conditioning plate is a rigid boundary and the conditioning compliance is a pressure release boundary.

The equivalent spectral density $\Phi_{vN}(\underset{\sim}{k},\omega)$ of the pressure in a turbulent boundary layer (TBL), as a function of $(k_x c/\omega)$ with $(k_y c/\omega) \equiv 0$.

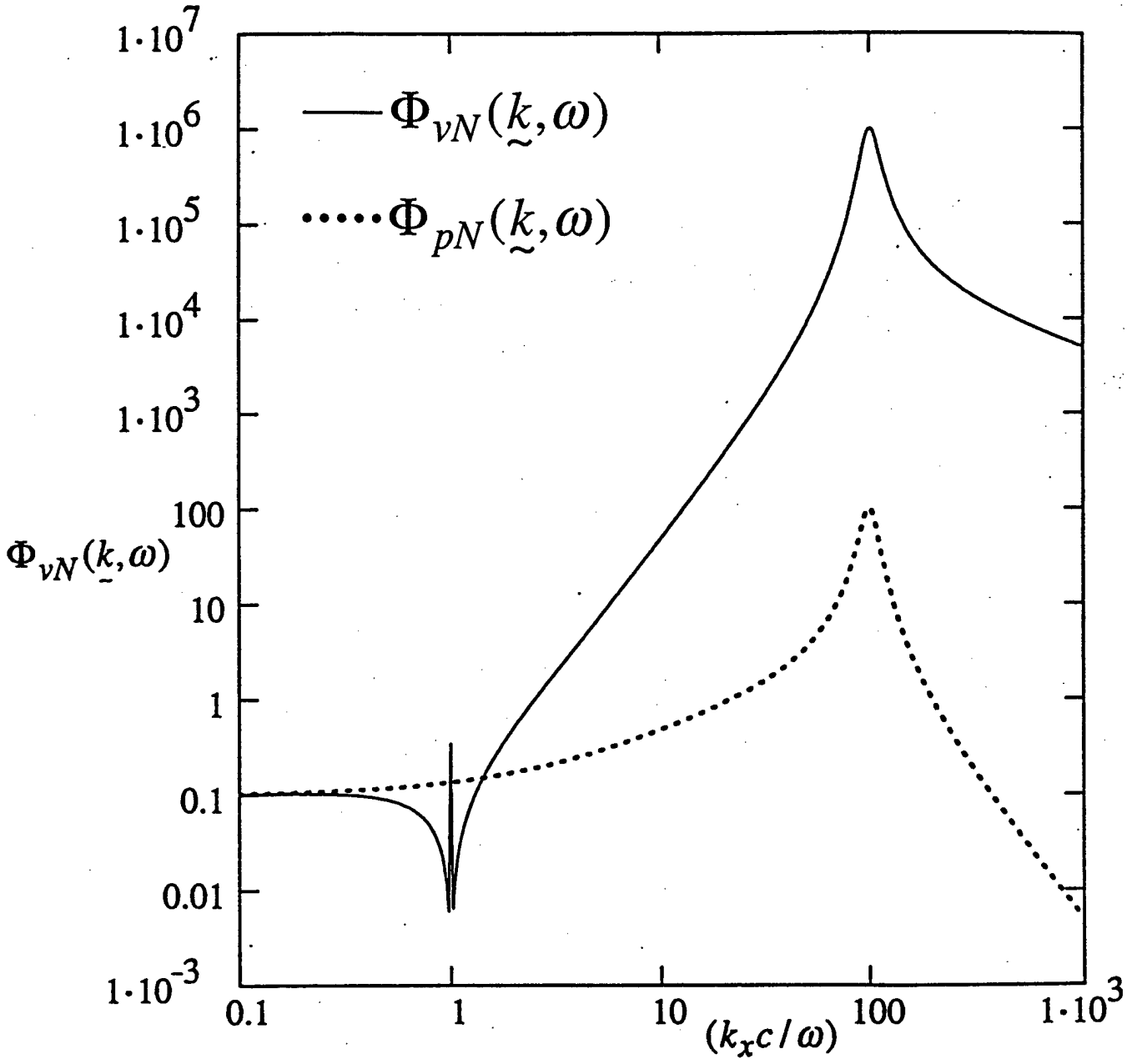

V.30a

Viewgraph 30b

As in Viewgraph 30a except that the comparison is made with respect to the cross stream-wise of a TBL. Again, the velocity array has to handle much more in the subsonic range.

The equivalent spectral density $\Phi_{vN}(\underset{\sim}{k},\omega)$ of the pressure in a turbulent boundary layer (TBL), as a function of $(k_y c/\omega)$ with $(k_x c/\omega) \equiv 0$.

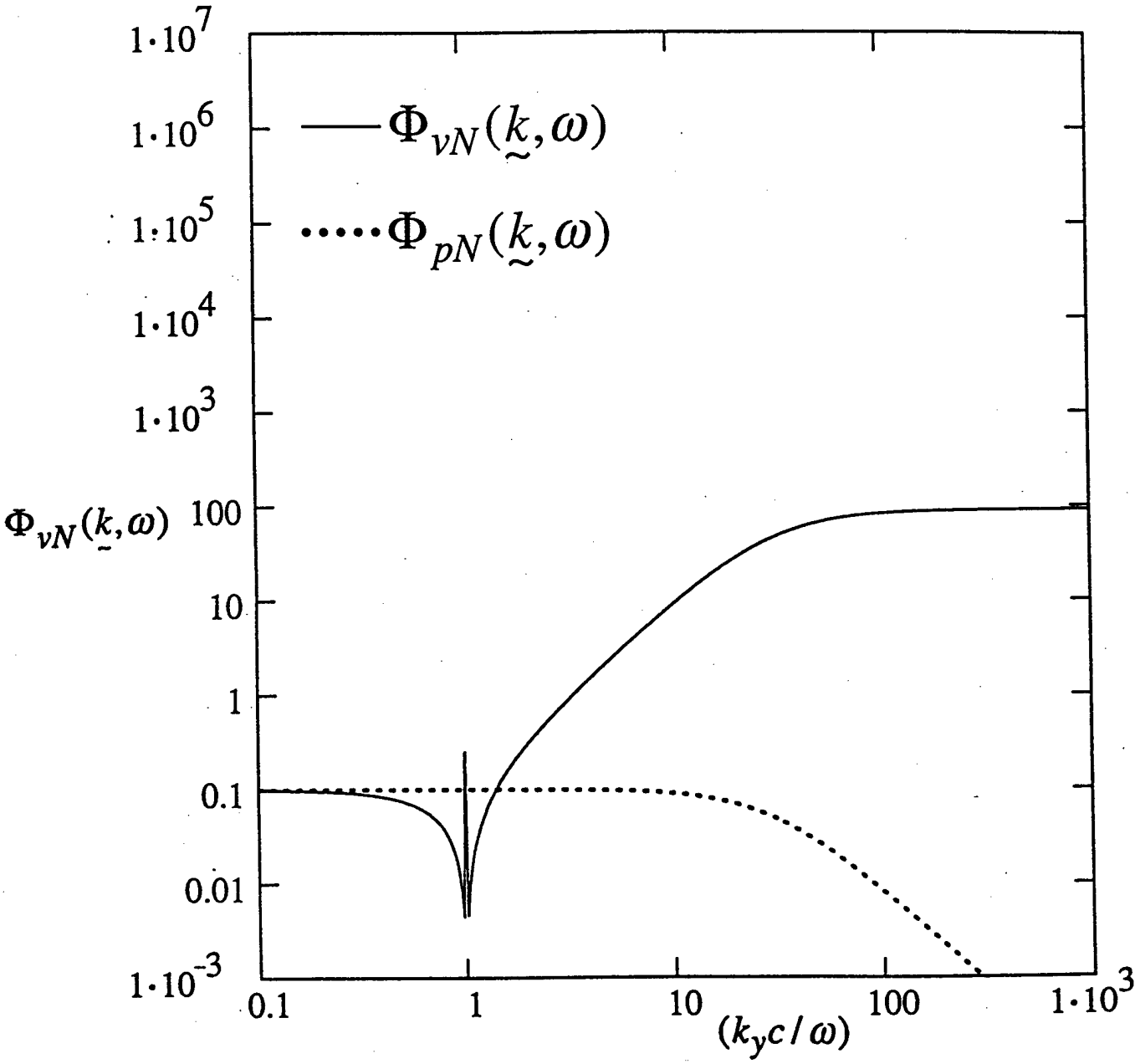

Viewgraph 31

The spectral density $\Phi_{vN}(\underset{\sim}{k},\omega)$ in the stream-wise of the noise in a TBL that an equivalent velocity array needs to handle versus the corresponding spectral density $\Phi_{pN}(\underset{\sim}{k},\omega)$ that a pressure array handles.

With these parameters the pressure array clearly wins inspite of the utilization of a resonance in the conditioning compliance at $(kc/\omega)_o = \sqrt{2}$.

The equivalent spectral density $\Phi_{vN}(\underset{\sim}{k},\omega)$ of the pressure in a turbulent boundary layer (TBL), as a function of $(k_x c/\omega)$ with $(k_y c/\omega) \equiv 0$. The parameters (ε_o) and (ε_c) are set equal to 10^0 and 10^{-1}, respectively, and $(\omega_c/\omega) = 6$.

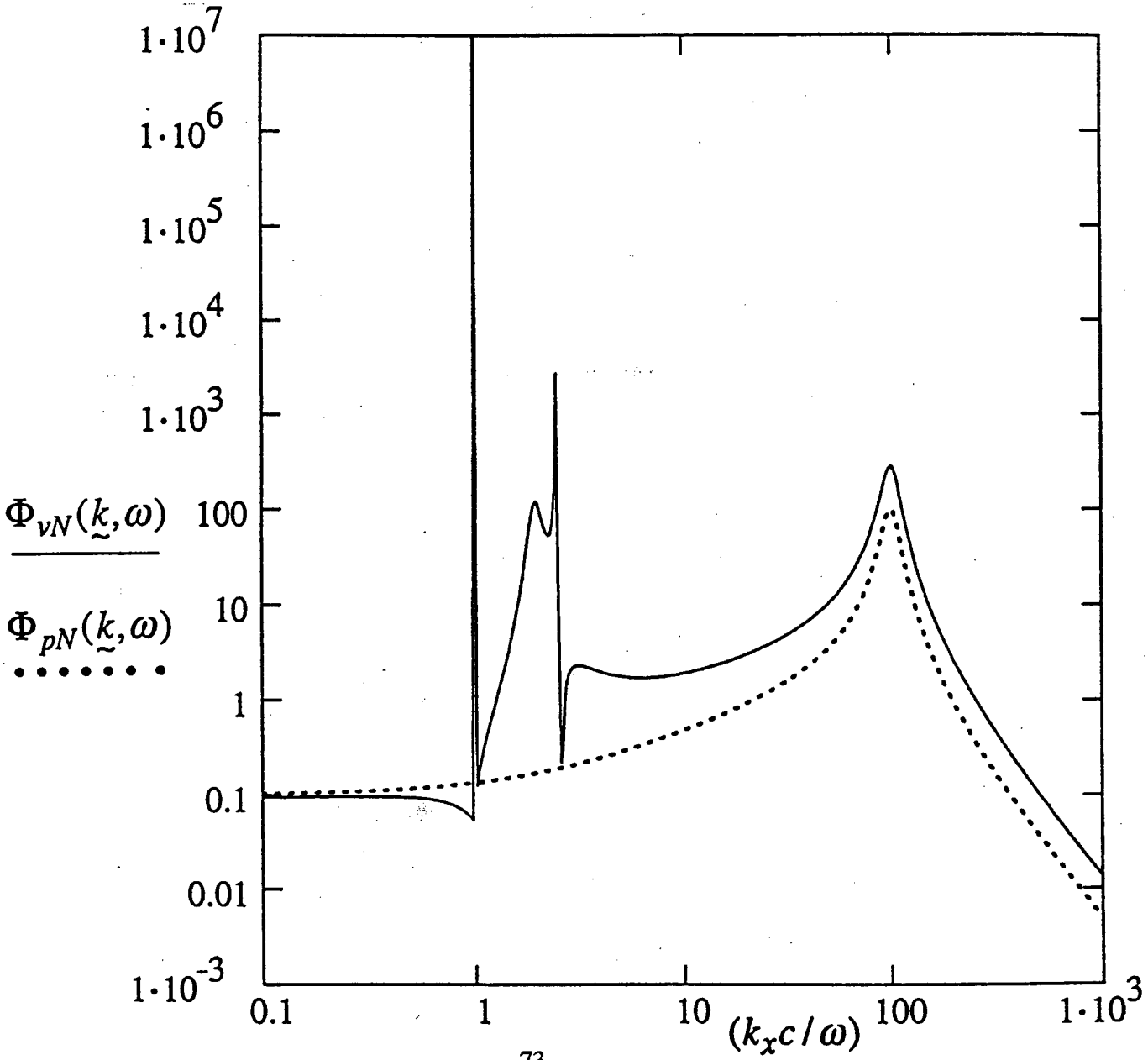

Viewgraph 32

With these parameters and with the exception of the narrow range in (kc/ω) about $(kc/\omega)_o$ the velocity array matches the filtering efficiency of the pressure array.

The equivalent spectral density $\Phi_{vN}(\underset{\sim}{k},\omega)$ of the pressure in a turbulent boundary layer (TBL), as a function of $(k_x c/\omega)$ with $(k_y c/\omega) \equiv 0$. The parameters (ε_o) and (ε_c) are set equal to 10^0 and 10^{-1}, respectively, and $(\omega_c/\omega) = 12$.

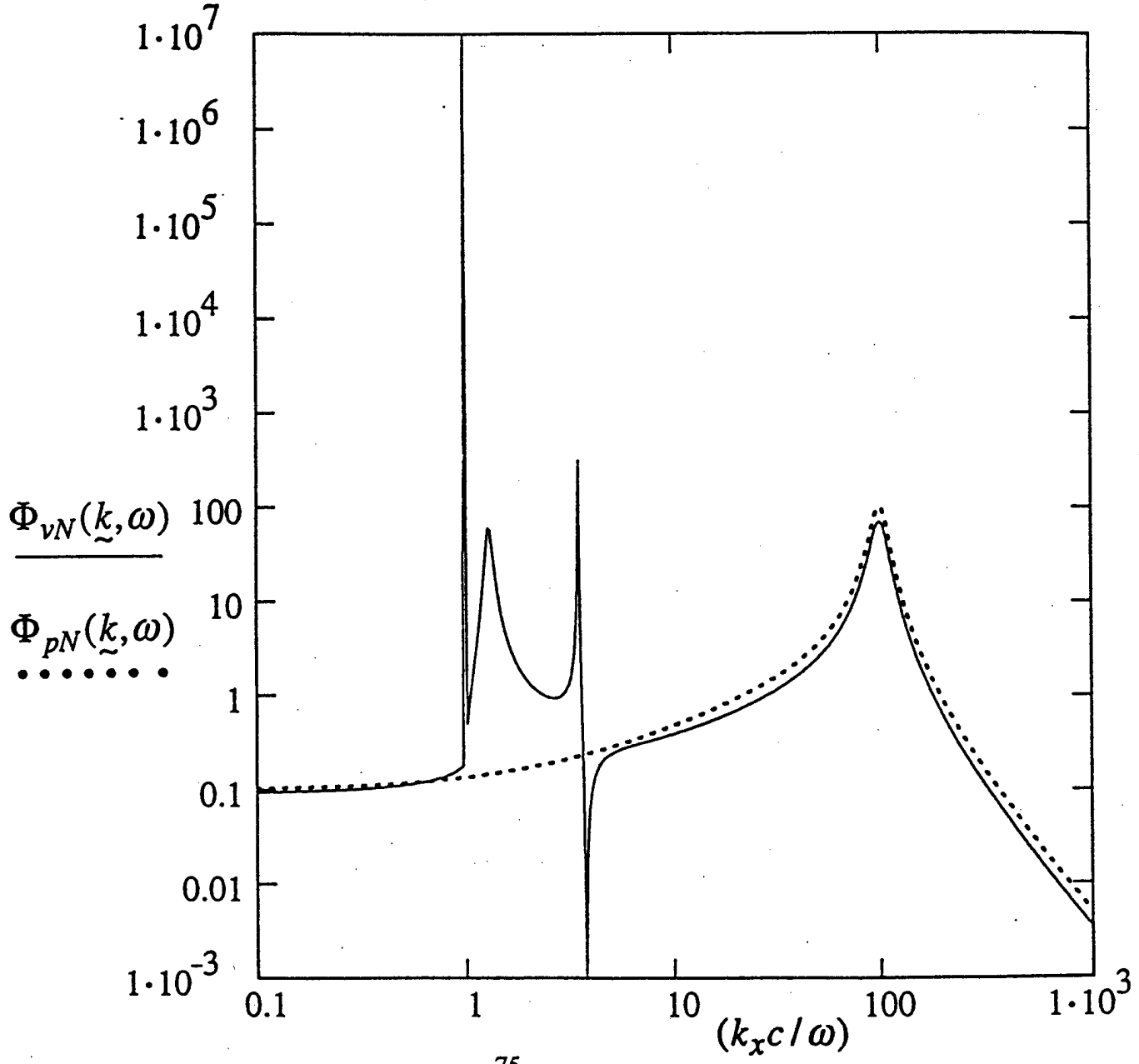

Viewgraph 33

With these parameters and with the exception of the narrow range in (kc/ω) centered about $(kc/\omega)_o$, the velocity array appears slightly but definitely better than the pressure array in handling the noise spectral density incident in the presence of a TBL.

The equivalent spectral density $\Phi_{vN}(\underset{\sim}{k},\omega)$ of the pressure in a turbulent boundary layer (TBL), as a function of $(k_x c/\omega)$ with $(k_y c/\omega) \equiv 0$. The parameters (ε_o) and (ε_c) are set equal to 10^0 and 10^{-1}, respectively, and $(\omega_c/\omega) = 18$.

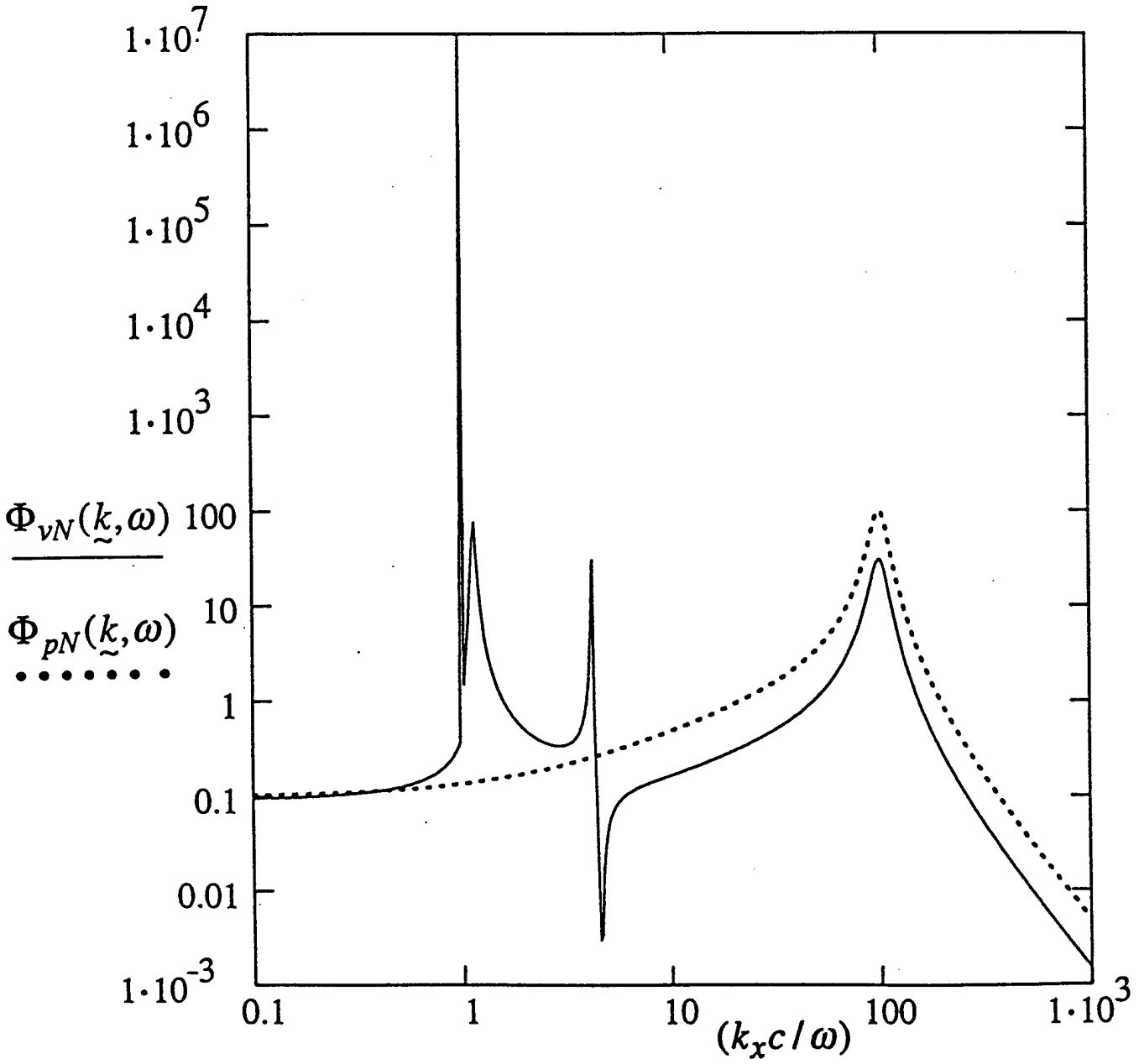

Viewgraph 34

A question that remains: Is the requirement for a conditioning compliance, that resonates at an appropriately chosen resonance frequency (ω_o), in the realm of practicality? The estimations conducted on this viewgraph suggest an affirmative answer.

Homogenous

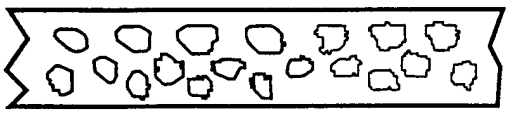

L

Discrete

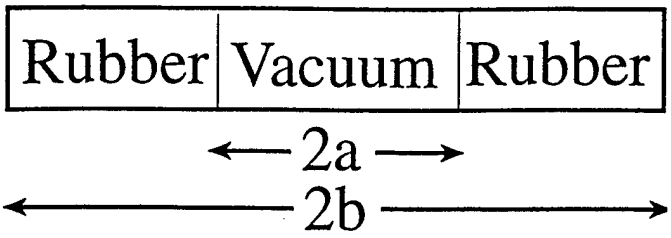

Surface stiffness $K = K_o(1+i\eta_o);\ K_o = (M_e / L)$

where $M_e(f)$ is the effective modulus which usually is a function of the frequency (f).

$M_e(f) = \rho_e c_e^2(f)$

$\rho_e = \rho[1-(V_o / V)]$

$M_e(f) = 3G(f)[1-(a/b)^2]$

$G(f) =$ shear modulus

Typically for $f \simeq 600(s)^{-1}$ and $(p_h / p_a) >> 1$

$\rho_e \simeq 0.6\rho \simeq 0.6(cgs)$

$c_e(600) \simeq c = 3.5x10^4(cm/s)$

$L = 2" \equiv 5.08(cm)$

$\boxed{K_o \simeq 1.44\ x\ 10^8(cgs)}$

$10^0 = \varepsilon_o = K_o(\omega_o \rho c)^{-1}$;

$\rho c = 3.5\ x\ 10^4(cgs)$

$[1-(a/b)^2] \simeq 0.856$

$M_e(600) \simeq 5.4\ x\ 10^7(cgs)$

$L \simeq 0.7(cm)$

$\boxed{K_o \simeq 7.7\ x\ 10^7(cgs)}$

$\omega_o = 2\pi\, x\, 6\ x\ 10^2(s)^{-1}$

$\boxed{K_o \simeq 1.3\ x\ 10^8(cgs)}$

REFERENCES*

1. G. Maidanik and K.J. Becker, "Primitive comparison of the signal-to-noise ratios of pressure and velocity planar arrays," NSWCCD-SIG-97/256-7030 (1997).

2. G. Maidanik and J. Dickey, "A boundary that sustains negligible reflection coefficient over a wide frequency band," NSWCCD-70-TR--1999/164 (1999).

3. G. Maidanik, "Surface-impedance nonuniformities as wave-vector convertors," Journal of the Acoustical Society of America **46**, 1062-1073 (1969).

*References in this report are in addition to those given in Reference 1.

INITIAL DISTRIBUTION

Copies	
3	NAVSEA 03T2 2 Taddeo 1 Biancardi
5	ONR/ONT 1 334 Tucker 1 334 Radlinski 1 334 Vogelsong 1 334 Main 1 Library
4	NRL 1 5130 Bucaro 1 5130 Williams 1 5130 Photiadis 1 Library
7	NUWC/NPT 2 Cray 1 Sandman 1 Harari 1 Boisvert 1 3332 Lee 1 Library
2	DTIC
2	Johns Hopkins University 1 Green 1 Dickey
4	ARL/Penn State University 1 Burroughs 1 Hwang 2 Hambric
1	Cambridge Collaborative Manning
1	Cambridge Acoustical Associate Garrelick
1	J. G. Engineering Research Greenspan
1	MIT 1 Dyer
1	Catholic Uni. Of Am. Eng. Dept. McCoy

Copies	
2	Boston University 1 Pierce 1 Barbone
2	Penn State University Koopman
2	Virginia Tech 1 Knight 1 Fuller

CENTER DISTRIBUTION

Copies	Code	Name
1	011	Corrado
2	0112	Douglas Halsall
1	20	
1	26	Everstine
1	6401	Castelli
1	70	Covich
4	7015	Fisher Sevik Hamly Vendittis
1	7020	Strasberg
3	7030	
2	7200	Niemiec Dlubac
2	7250	Shang Maga
1	842	Graesser
2	3421	(TIC-Carderock)